










Article

Multipotent Cholinesterase Inhibitors for the Treatment of Alzheimer's Disease: Synthesis, Biological Analysis and Molecular Docking Study of Benzimidazole-Based Thiazole Derivatives

Rafaqat Hussain ¹, Hayat Ullah ^{2,*} , Fazal Rahim ^{1,*}, Maliha Sarfraz ³, Muhammad Taha ⁴ , Rashid Iqbal ⁵ , Wajid Rehman ¹ , Shoaib Khan ¹, Syed Adnan Ali Shah ^{6,7} , Sajjad Hyder ⁸ , Majid Alhomrani ^{9,10} , Abdulhakeem S. Alamri ^{9,10} , Osama Abdulaziz ⁹ and Mahmoud A. Abdelaziz ¹¹ 

¹ Department of Chemistry, Hazara University, Mansehra 21120, Pakistan

² Department of Chemistry, University of Okara, Okara 56300, Pakistan

³ Department of Zoology, Wildlife and Fisheries, University of Agriculture Faisalabad, Sub-Campus Toba Tek Singh, Punjab 36050, Pakistan

⁴ Department of Clinical Pharmacy, Institute for Research and Medical Consultations (IRMC), Imam Abdulrahman Bin Faisal University, P.O. Box 1982, Dammam 31441, Saudi Arabia

⁵ Department of Agronomy, Faculty of Agriculture and Environment, The Islamia University of Bahawalpur Pakistan, Bahawalpur 63100, Pakistan

⁶ Faculty of Pharmacy, Universiti Teknologi MARA Cawangan Selangor Kampus Puncak Alam, Bandar Puncak Alam 42300, Selangor, Malaysia

⁷ Atta-ur-Rahman Institute for Natural Product Discovery (AuRIns), Universiti Teknologi MARA Cawangan Selangor Kampus Puncak Alam, Bandar Puncak Alam 42300, Selangor, Malaysia

⁸ Department of Botany, Government College Women University, Sialkot 51310, Pakistan

⁹ Department of Clinical Laboratories Sciences, The Faculty of Applied Medical Sciences, Taif University, Taif 21944, Saudi Arabia

¹⁰ Centre of Biomedical Sciences Research (CBSR), Deanship of Scientific Research, Taif University, Taif 21944, Saudi Arabia

¹¹ Department of Chemistry, Faculty of Science, University of Tabuk, P.O. Box 741, Tabuk 71491, Saudi Arabia

* Correspondence: ayaanwazir366@gmail.com (H.U.); fazalstar@gmail.com (F.R.)



Citation: Hussain, R.; Ullah, H.; Rahim, F.; Sarfraz, M.; Taha, M.; Iqbal, R.; Rehman, W.; Khan, S.; Shah, S.A.A.; Hyder, S.; et al. Multipotent Cholinesterase Inhibitors for the Treatment of Alzheimer's Disease: Synthesis, Biological Analysis and Molecular Docking Study of Benzimidazole-Based Thiazole Derivatives. *Molecules* **2022**, *27*, 6087. <https://doi.org/10.3390/molecules27186087>

Academic Editor: Athina Geronikaki

Received: 7 August 2022

Accepted: 5 September 2022

Published: 18 September 2022

Publisher's Note: MDPI stays neutral with regard to jurisdictional claims in published maps and institutional affiliations.



Copyright: © 2022 by the authors. Licensee MDPI, Basel, Switzerland. This article is an open access article distributed under the terms and conditions of the Creative Commons Attribution (CC BY) license (<https://creativecommons.org/licenses/by/4.0/>).

Abstract: Twenty-four analogues of benzimidazole-based thiazoles (**1–24**) were synthesized and assessed for their in vitro acetylcholinesterase (AChE) and butyrylcholinesterase (BuChE) inhibitory potential. All analogues were found to exhibit good inhibitory potential against cholinesterase enzymes, having IC₅₀ values in the ranges of 0.10 ± 0.05 to 11.10 ± 0.30 μM (for AChE) and 0.20 ± 0.050 μM to 14.20 ± 0.10 μM (for BuChE) as compared to the standard drug Donepezil (IC₅₀ = 2.16 ± 0.12 and 4.5 ± 0.11 μM, respectively). Among the series, analogues **16** and **21** were found to be the most potent inhibitors of AChE and BuChE enzymes. The number (s), types, electron-donating or -withdrawing effects and position of the substituent(s) on the both phenyl rings B & C were the primary determinants of the structure-activity relationship (SAR). In order to understand how the most active derivatives interact with the amino acids in the active site of the enzyme, molecular docking studies were conducted. The results obtained supported the experimental data. Additionally, the structures of all newly synthesized compounds were elucidated by using several spectroscopic methods like ¹³C-NMR, ¹H-NMR and HR EIMS.

Keywords: Synthesis; acetylcholinesterase; butyrylcholinesterase; benzimidazole; thiazole; structure-activity relationship; molecular docking

1. Introduction

Alzheimer's disease (AD) is a complex neurodegenerative and irretrievable abnormality. Its pathology involves the interactions of genetic risk and environmental factors [1]. This disease is considered age-related because it is the main cause of dementia, and is

frequently found in old people. AD was counted as the fourth major death-causing disease in developed countries, after cancer, cerebral disease and cardiovascular disease [2]. Thus, it affects cholinergic neurons as well as cholinergic transmission. Moreover, AD is a multi-pathogenic illness; therefore, the recent strategy in drug discovery is to synthesize novel and potent anti-Alzheimer agents with significant inhibition potential for acetylcholinesterase (AChE) and butyrylcholinesterase (BuChE) enzymes [3]. Acetylcholine is crucial for cognitive processes, including memory. It lessens cholinergic neurotransmission in the brain, a factor that is significant in the cognitive decline brought on by Alzheimer's disease [4,5]. BuChE is an enzyme related to AChE, and BuChE has been attracting growing attention due to its positive role in AD [6,7]. Butyrylcholinesterase prevents an enzyme from interfering with neurotransmitter transmission, which results in side effects for patients include nausea, vomiting, fever, and even death [8,9]. Thus, it might be considered as a significant tool for novel drug synthesis and used as the best target to treat AD. Therefore, the future development of potent BuChE inhibitors, as well as the regular practice of cholinesterase inhibitors, may lead to facilitating clinical results [10].

Benzimidazole possesses a diverse range of biological activities, such as anti-histaminic, anti-convulsant, anti-analgesic, proton pump inhibitors, anti-hypertensive, anti-cancer, antiviral, anti-fungal and anti-coagulant actions [11–17]. There are some drug molecules such as benoxaprofen, albendazole, envirodin, bendamustine, omeprazole and astemizole that contain a benzimidazole moiety in their skeleton (Figure 1) [18].

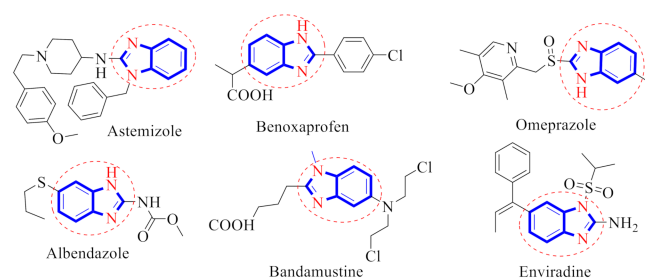


Figure 1. Drugs containing abenzimidazole skeleton.

Thiazoles scaffolds were recognized to play an essential role in the field of medicines. Thiazoles and their analogues were reported to have anti-Alzheimer's, anti-diuretic and anti-bacterial activities [19]. Moreover, thiazole-based hybrids have promising medicinal applications, including analgesic, anti-inflammatory [20], anti-microbial [21], anti-cancer [22], anti-hypoxic [23], anti-asthmatic [24] and anti-hypertensive activities [25]. In addition, thiazole derivatives and their chromene-based hybrids have demonstrated potent AChE-inhibitory activity [26–29]. Furthermore, it was reported that due to the broad range of pharmacological significance of thiazole, a large number of commercially available drugs contain a thiazole nucleus in their structure, including abafungin, niridazole, tiabendazole, ruviconazole, vorelaxin and azereonam (Figure 2) [30,31].

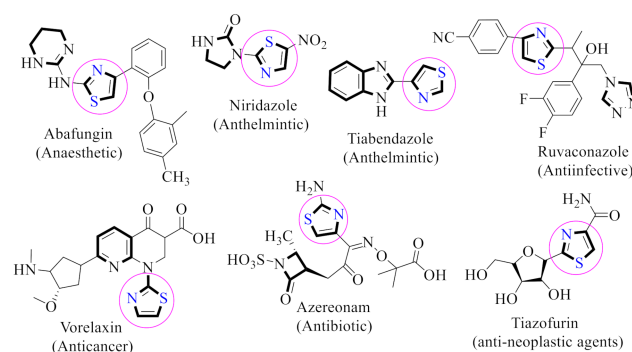


Figure 2. Bioactive drugs with a thiazole skeleton.

Our research group had identified different classes of heterocyclic compounds as potent inhibitors [32–41]. Moreover, we had already reported on the anti-AChE and anti-BuChE activities of benzimidazole [42] and thiazole [43] derivatives (Figure 3). Keeping in view the biological significance of thiazole and benzimidazole skeleton containing analogues [44,45], here in this study, hybrid analogues of benzimidazole-based thiazole were designed and synthesized (1–24) as potent inhibitors of acetylcholinesterase and butyrylcholinesterase.

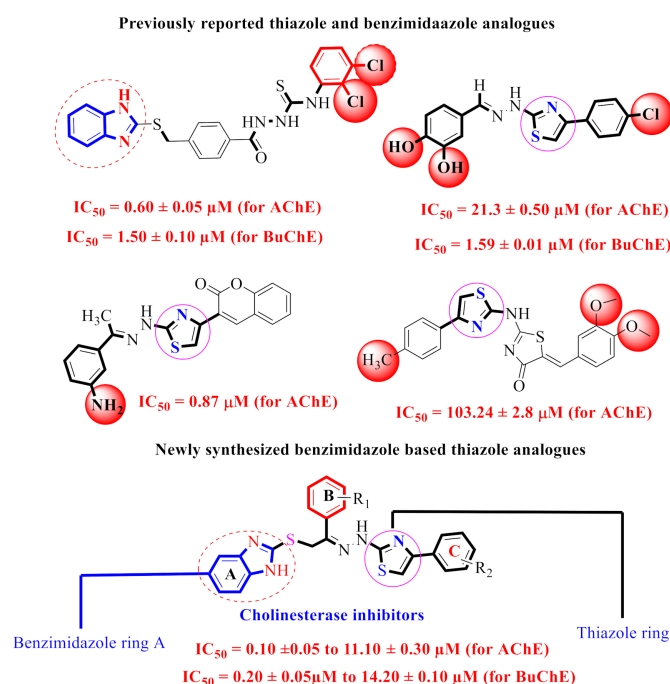


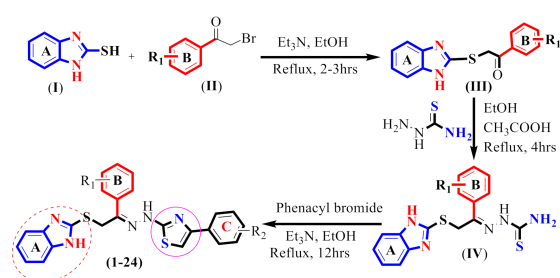
Figure 3. Rationale of the current study.

2. Results and Discussion

2.1. Chemistry

In this study, well-known methodology was adopted for the synthesis of benzimidazole-based thiazole derivatives (1–24) from readily accessible precursors such thiosemicarbazide, various phenacyl bromides and 2-mercaptobenzimidazole.

Initially, 2-bromoacetophenone (II) was reacted with 2-mercapto benzimidazole (I) in EtOH and Et₃N (catalyst), and the reaction mixture was refluxed for 2–3 h to yield the first intermediate (III) [44]. An equivalent amount of intermediate (III) and thiosemicarbazide were further treated in EtOH and CH₃COOH (glacial) and the solution was refluxed for about 4 h to yield a second intermediate product (IV). The reaction mixture was cooled to room temperature when it was finished, and the precipitate solid that resulted was then filtered and washed with n-hexane. The reaction's progress had been monitored by using TLC plate. Finally, intermediate (IV) underwent cyclization with stirring overnight with a different substituted 2-bromoacetophenone in EtOH and Et₃N (catalyst) to yield benzimidazole-based thiazole analogues (1–24) in moderate to good yield (Scheme 1). The solvent was removed after being cooled to 25 °C and the resultant solid residue was then cleaned by washing with n-hexane and re-crystallized from ethyl acetate. The precise structures of all newly synthesized analogues were determined using several spectroscopic methods, including ¹³C-NMR, ¹H-NMR and HR EIMS.



Scheme 1. Synthesis of benzimidazole-based thiazole derivatives (1–24).

The ^1H NMR spectrum of analogue **1** was recorded in $\text{DMSO-}d_6$ on a Bruker 600 MHz instrument. The peak for the hydroxyl proton (OH) was observed at δ_{H} 10.11 (s, 1H, -OH). The most downfield singlets of two -NH protons, one for benzimidazole (NH) and another amino (NH) proton between the thiazole and benzimidazole rings, were resonated at δ_{H} 13.25 and 11.81, respectively. The molecule comprises three aromatic rings labeled as A, B C. Among the ring B protons, doublets appeared at δ_{H} 7.79 for two protons H-2' and H-6' (Ar-H), while another two protons of this ring H-3' H-5' (Ar-H) were resonated at δ_{H} 7.88 (d, $J = 8.88$ Hz, 2H, Ar-H) as doublets, respectively. On the other hand, two aromatic protons labeled as H-3'' and H-6'' (Ar-H) of ring C resonated at δ_{H} 8.28 (s, 1H, H-3'') and 8.10 (s, 1H, H-6'') as singlets. Besides this, a triplet was observed for two aromatic protons of benzimidazole at δ_{H} 7.43 (t, $J = 7.92$ Hz, 2H, H-5/H-6). However, thiazole-H was resonated at δ_{H} 7.33 as a singlet. Moreover, two more aromatic protons of benzimidazole, namely H-4 and H-7, were also resonated as doublets at δ_{H} 7.27 (d, $J = 7.68$ Hz, 1H, H-4) and 7.04 (d, $J = 7.56$ Hz, 1H, H-7), respectively. Furthermore, a singlet was also observed for two active methylene protons (-CH₂-) attached between sulfur and aromatic ring B at δ_{H} 2.34 (s, 2H, -S-CH₂).

As for compound **1**, the ^{13}C NMR signal $\delta_{\text{C-13}}$ at 175.81 was attributed to a thiazole carbon (C) present between sulfur and nitrogen atoms, while two peaks at $\delta_{\text{C-13}}$ 139.85 (C-thiazole) and 110.66 (C-thiazole) were observed for the remaining two carbons of the thiazole ring. The peak at $\delta_{\text{C-13}}$ 138.96 (C) was observed for the benzimidazole carbon-bearing substitution, while two bridged carbons of benzimidazole were recorded at $\delta_{\text{C-13}}$ 137.27 (C). The carbon involved in the doublet with nitrogen (C=N) was resonated at $\delta_{\text{C-13}}$ 143.52 (C). The carbons of the aromatic phenyl rings B and C involving substitutions were resonated at $\delta_{\text{C-13}}$ 133.67 (C-OH), 132.00 (C-NO₂), 127.83 (C), 126.25 (C-Cl) and 125.92 (C-Br). The peak corresponding to carbons of aromatic rings B and C without substitutions were resonated at $\delta_{\text{C-13}}$ 122.93 (CH-3' and CH-5'), 123.69 (CH), 120.66 (CH-2' and CH-6') and 119.01 (CH), respectively. The peaks corresponding to the remaining four carbons of benzimidazole were observed at $\delta_{\text{C-13}}$ 123.7 (CH), 123.5 (CH), 115.8 (CH) and 115.3 (CH), respectively. The peak at $\delta_{\text{C-13}}$ 38.5 (-CH₂-) corresponded to active methylene groups attached to a sulfur atom.

2.2. In Vitro Evaluation of AChE and BChE Inhibition by Novel Benzimidazole-Based Thiazoles

All the newly synthesized derivatives of benzimidazole-based thiazole (1–24) were evaluated as potential inhibitors of AChE and BChE, and IC_{50} was determined. All analogues showed moderate to good inhibitory potential against both AChE and BChE. The IC_{50} values ranged from 0.10 ± 0.05 – 11.10 ± 0.30 μM (for AChE) and 0.20 ± 0.050 – 14.20 ± 0.10 μM (for BChE). Some of these compounds were shown to be more potent inhibitors than the standard drug Donepezil ($\text{IC}_{50} = 2.16 \pm 0.12$ μM and 4.5 ± 0.11 μM respectively) (Table 1). The synthesized analogue was divided into four parts: benzimidazole ring A, thiazole portion, phenyl rings B & C, in order to better understand the structure-activity relationship (SAR). The nature, electron-withdrawing or -donating effects, number(s) and position of the substituent(s) on both phenyl rings B and C respectively were measured to be the key determinants of the structure-activity relationship (Figure 4).

Table 1. IC₅₀ values and selectivity index values of tested benzimidazole-based thiazole derivatives determined for AChE and BuChE.

S.NO	Ring B	Ring C	IC ₅₀ AChE	IC ₅₀ BuChE	Selectivity Index
1			4.60 ± 0.10	7.60 ± 0.10	1.65
2			2.30 ± 0.10	3.20 ± 0.10	0.9
3			0.80 ± 0.10	1.80 ± 0.10	2.25
4			3.50 ± 0.10	5.30 ± 0.10	1.51
5			8.60 ± 0.20	10.70 ± 0.20	1.24
6			0.70 ± 0.05	1.40 ± 0.05	2.0
7			2.90 ± 0.10	3.50 ± 0.10	1.21

Table 1. Cont.

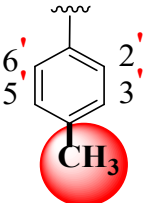
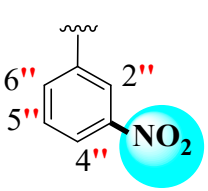
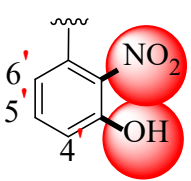
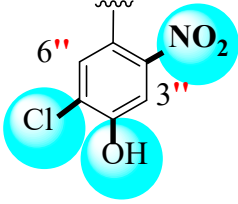
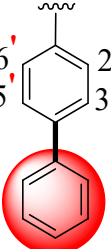
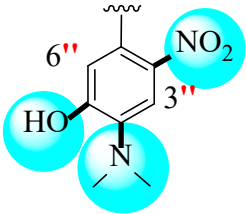
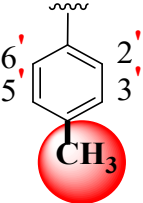
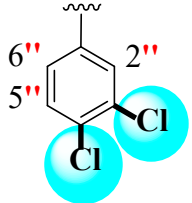
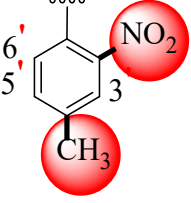
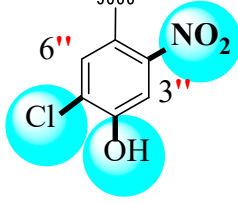
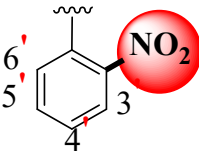
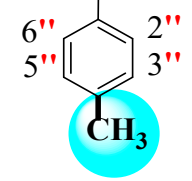
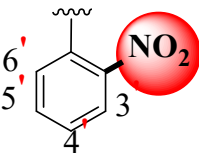
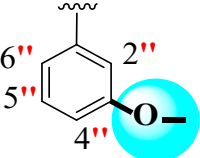
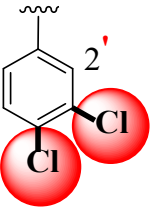
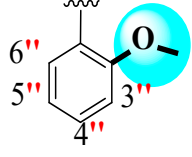
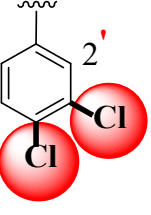
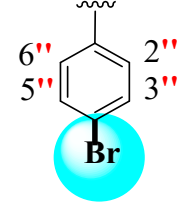
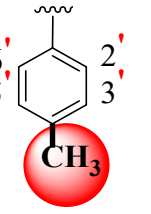
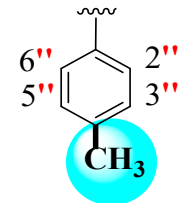
S.NO	Ring B	Ring C	IC ₅₀ AChE	IC ₅₀ BuChE	Selectivity Index
8			6.30 ± 0.10	7.90 ± 0.10	1.25
9			1.30 ± 0.10	3.20 ± 0.10	2.46
10			N.A.	N.A.	-
11			0.40 ± 0.050	1.10 ± 0.10	2.75
12			1.40 ± 0.10	2.10 ± 0.10	1.5
13			3.20 ± 0.10	5.10 ± 0.10	1.59
14			3.10 ± 0.10	4.20 ± 0.10	1.35

Table 1. Cont.

S.NO	Ring B	Ring C	IC ₅₀ AChE	IC ₅₀ BuChE	Selectivity Index
15			0.30 ± 0.050	0.70 ± 0.050	2.33
16			0.20 ± 0.050	0.50 ± 0.050	2.5
17			1.10 ± 0.050	1.80 ± 0.10	1.64
18			0.70 ± 0.050	1.20 ± 0.10	1.71
19			1.40 ± 0.10	1.30 ± 0.10	0.92
20			1.20 ± 0.10	1.90 ± 0.10	1.58
21			0.10 ± 0.05	0.20 ± 0.05	2.0

Table 1. Cont.

S.NO	Ring B	Ring C	IC ₅₀ AChE	IC ₅₀ BuChE	Selectivity Index
22			0.40 ± 0.20	0.70 ± 0.10	1.75
23			4.70 ± 0.10	6.70 ± 0.10	1.43
24			11.10 ± 0.30	14.20 ± 0.10	1.28
Standard drug Donepezil			2.16 ± 0.12 μM	4.5 ± 0.11 μM	2.08

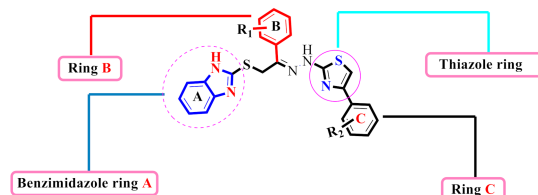


Figure 4. General structure of benzimidazole-bearing 1,3-thiazole scaffolds (1–24).

Structure–Activity Relationship of acetylcholinesterase and butyrylcholinesterase activities

The derivative **21** (IC₅₀ = 0.10 ± 0.05 μM and 0.20 ± 0.05 μM), bearing di-Cl groups at *meta*- and *para*-positions of both phenyl rings **B** and **C** correspondingly, was emerged as most effective inhibitors of both targeted enzymes (AChE & BuChE). Additionally, the analogue **16** (IC₅₀ = 0.20 ± 0.050 μM for AChE) and 0.50 ± 0.050 μM for BuChE), which had a hydroxy group at the *para*-position of phenyl ring **C** and a nitro group at the *ortho*-position of phenyl ring **B** was found to be the 2nd most potent inhibitor of both AChE & BuChE enzymes. The different types, number (s), electron-donating or -withdrawing effect, positions of substituent(s) on the both phenyl rings **B** and **C** may account for the effective inhibitory potentials of analogues **16** and **21** (Figure 5).

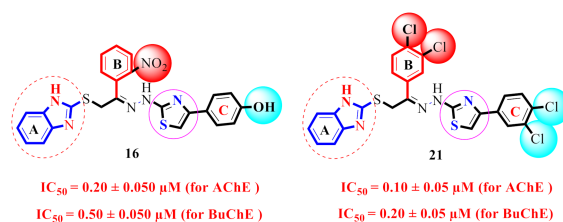


Figure 5. SAR study of the most active scaffolds.

By comparing compounds 3–6 (Figure 6), we noticed that there is a difference in the inhibitory potential of these compounds in regard to the position of the substituent(s). This may be caused by the type, position, and number(s) of the substituent(s) on ring C.

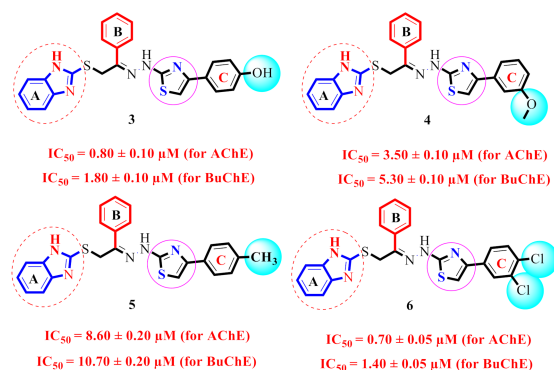


Figure 6. SAR study of scaffolds 3–6.

Analogue 11 (dichloro group at *meta*- and *para*-positions on ring C, $IC_{50} = 0.40 \pm 0.050 \mu\text{M}$ and $1.10 \pm 0.10 \mu\text{M}$) was found to be superior to analogues 7 (nitro group at *ortho* on ring C, $IC_{50} = 2.90 \pm 0.10 \mu\text{M}$ and $3.50 \pm 0.10 \mu\text{M}$) and 8 (nitro group at *meta* position on ring C, $IC_{50} = 6.30 \pm 0.10 \mu\text{M}$ and $7.90 \pm 0.10 \mu\text{M}$) (Figure 7).

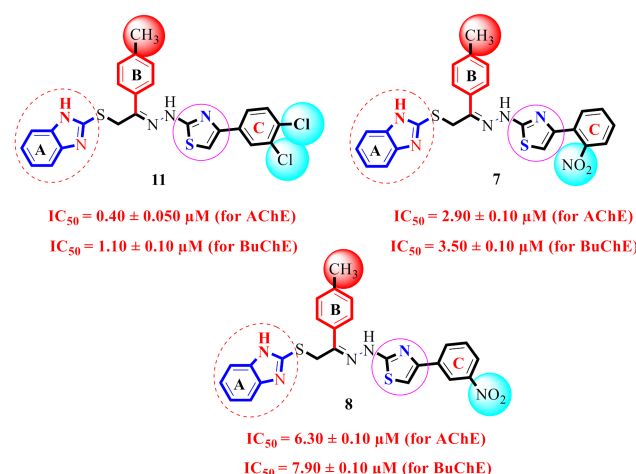


Figure 7. SAR study of scaffolds 7, 8 and 11.

By comparing compounds 13–16 (Figure 8), we noticed that there is a difference in the inhibitory potentials of these compounds in regard to the position of the substituent(s). This could be due to the nature of the substituent(s) on ring C.

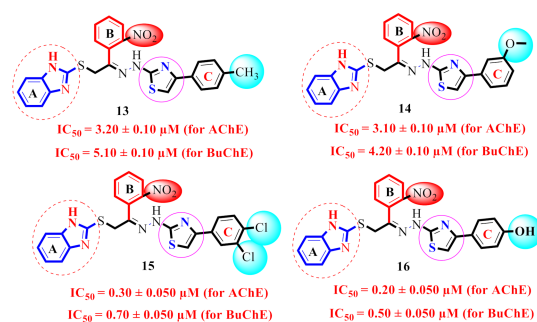


Figure 8. SAR study of scaffolds 13–16.

By comparing compounds 17–19 and 21–22 (Figure 9), we noticed that there is a difference in the inhibitory potentials of these compounds in regard to the position of the substituent(s). This may be caused by the type, position, and number(s) of the substituent(s) on ring C.

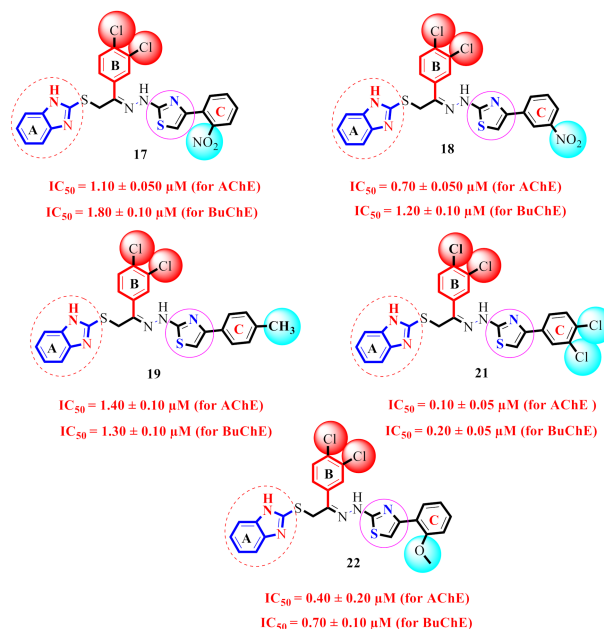


Figure 9. SAR study of scaffolds 17, 18, 19, 21 and 22.

Overall, it was found that the nature, electron-donating or -withdrawing effect, number and position of the substituent(s) on both rings B and C may considerably affect the inhibitory potentials of the synthesized analogues.

Galantamine is a phenanthrene that induces reversible inhibition of AChE-BuChE; Donepezil is a piperidine that causes reversible AChE inhibition, highly specific; and huperzine A is a pyridine that causes reversible AChE and specific inhibition. Under ideal test circumstances, each AChEI is ranked in the following order by its inhibitory efficacy (IC₅₀) against the AChE activity: physostigmine (0.67 nM) > rivastigmine (4.4 nM) > Donepezil (6.7 nM) > TAK-147 (12 nM) > tacrine (77 nM) > ipidacrine (270 nM). Based on study conducted by Eisai scientists, derivatives with 4-aminopyridine such as ipidacrine and tacrine did not exhibit any selectivity, benzylpiperidine derivatives including TAK-147 and Donepezil exhibited high selectivity for AChE over BuChE, while the carbamate derivatives exhibited moderate selectivity. AChE inhibition by Donepezil is 40–500 times more effective than by galantamine, according to more recent studies. Galantamine leaves the brain more quickly than Donepezil does. Galantamine and Donepezil both inhibit brain AChE to a similar degree, according to their respective K_i values, which are 7.1–19.1 and 0.65–2.3 g/g in different species, respectively, the doses of needed for galantamine is 3–15 times greater than those of Donepezil [46].

2.3. Docking Study

The main objective of molecular docking study was to learn more about how newly afforded compounds bind to enzymes (i.e., both AChE and BuChE). Based on the residing co-crystal of each crystallographic structure, all of the compounds were docked. Each compound received a total of thirty conformations before the docking process. For additional protein-ligand interaction (PLI) profiling, the top-ranked conformations were chosen.

The docking results showed that all of the compounds were located in the active sites of both enzymes in the proper orientation. In general, we found that all the compounds had different substitution groups at their two ends, while the third end remained the same for all compounds, i.e., the electron-donating groups (also known as activated groups) and

electron-withdrawing (also known as deactivated groups) at different positions. Additionally, we noticed that most active compounds held both the activated and deactivated groups at their two ends, which had a strong magnitude of activation. Surprisingly, the PLI profiles along with the in-vitro data revealed that compounds **16** and **21**, which contain activated and deactivated substituting groups over the benzene ring, had the highest inhibitory potential levels of the entire series. For example, compounds **16** and **21** have nearly identical activity levels against AChE but are ranked 1st **21** and 2nd **16** against BuChE, respectively.

Numerous significant interactions with catalytic residues were found in the comprehensive PLI profiles of both compounds against both targets. These interactions may have a significant impact on the improvement of the enzymatic activity of both enzymes. It was shown by PLI profile that analogue **21** adopted numerous key interactions with catalytic residues of AChE including the residues Phe330, Phe331, Tyr334, Asp72, Trp84, Tyr121 and Trp279 (Figure 10A), while this analogue against BuChE exhibited several important interactions such as Tyr332, Phe329, Ala328, Trp82, Asp70, Gly116, Gly117, Trp231, Ser287 and Leu286 (Figure 10B). The attached di-Cl on both ends of the compound may be the cause of its high potential, where the Cl that withdraw most of the electronic density from benzene ring, resulting in a partial positive charge over the benzene ring, causing this benzene ring to try to re-gain the stability via adopting several key interactions with active side residues, thereby enhancing the enzymatic activity. Overall, we observed that the compounds holding the substituted group, which had a strong magnitude of either withdrawal or donation, showed best potential against both targeted enzymes.

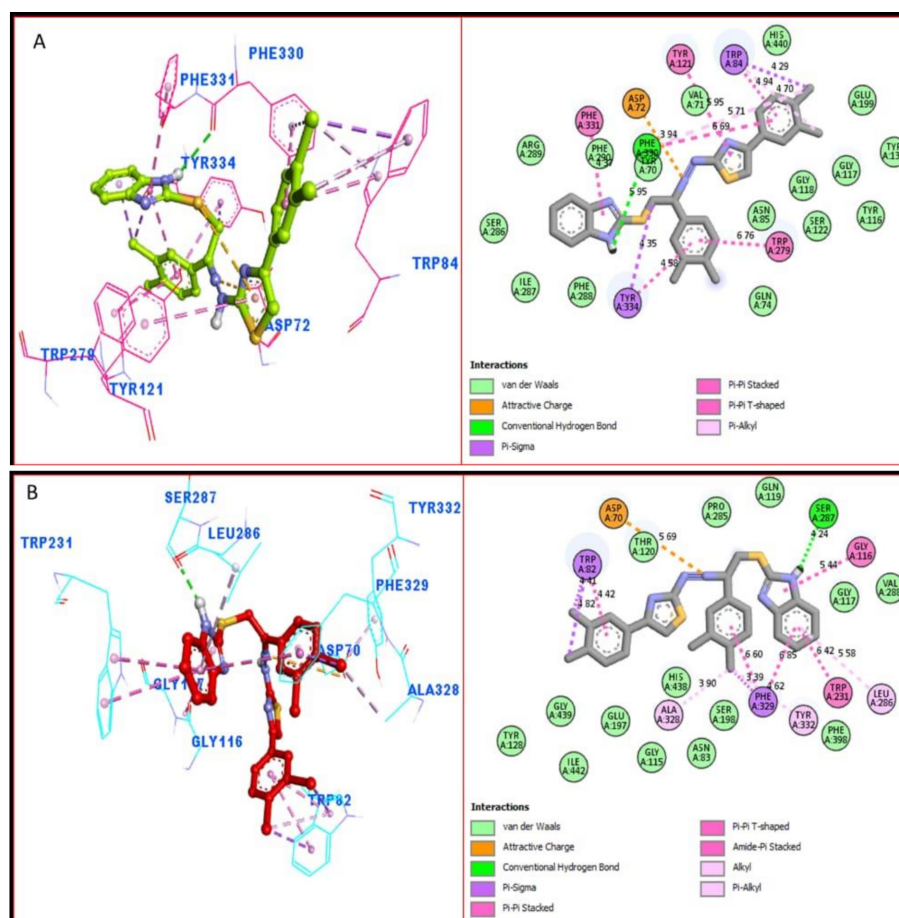


Figure 10. The PLI profile of the most potent analogue (**21**): **(A)** analogue **21** against acetylcholinesterase (AChE); **(B)** analogue **21** against butyrylcholinesterase (BuChE) enzymes.

Similarly, the PLI profile shown by analogue **16** against AChE revealed several key interactions with the active site residues, including the residues Trp84, Glu199, Tyr121, Trp279, Asp285, Tyr334 and Asp72 (Figure 11C), while against the BuChE, this compound adopted several key interactions with Trp231, Leu286, Pro285, Phe329, Asp70, Ile69, Ala328 and Trp82 (Figure 11D). The elevated potential of this compound may be a result of the strong electron-donating and electron-withdrawing groups that are connected to it, i.e., hydroxyl and nitro group, where the -OH-substituting group donates some its electronic density with high potential to the 6c-ring and then further this electronic density cascades to other important moieties of the compounds; hence, In this manner, the overall potency of compound as an inhibitor against both targeted enzymes is high. In addition, the PLI profile revealed several key interactions, particularly with the side of the attached substituted groups or nearby moieties.

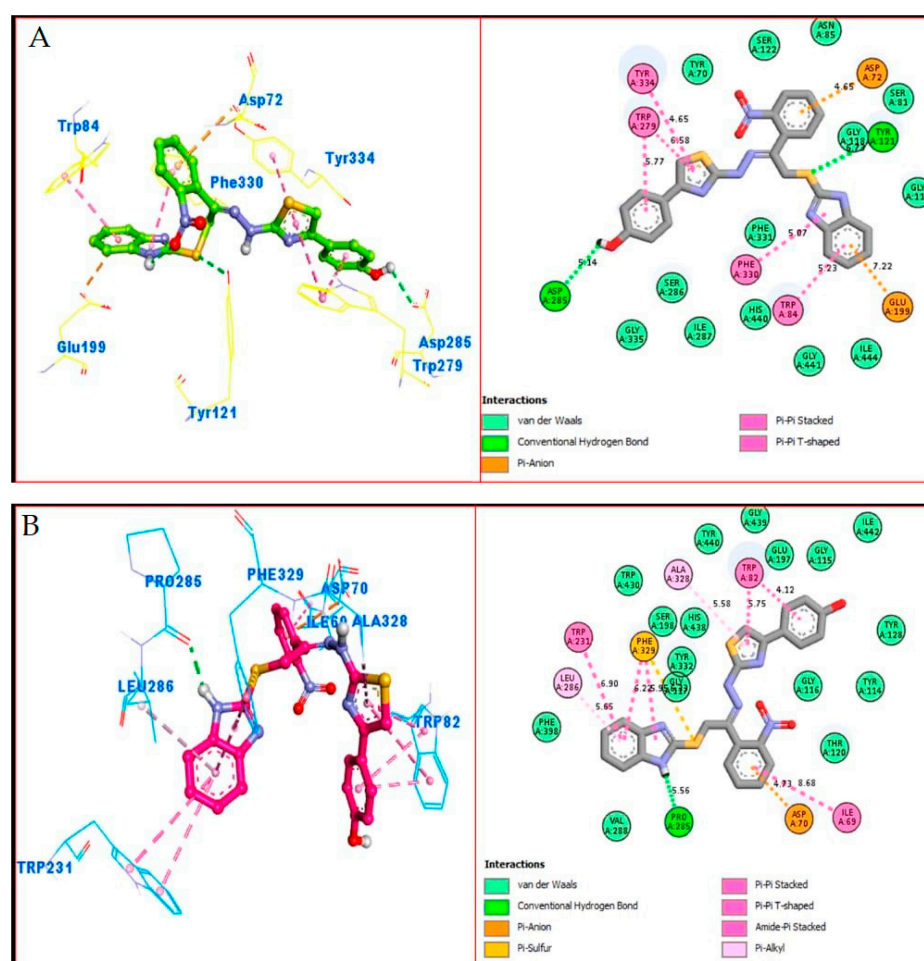


Figure 11. The PLI profile of second most potent analogue (**16**): (A) analogue **16** against acetylcholinesterase (AChE); (B) analogue **16** against butyrylcholinesterase (BuChE) enzymes.

Additionally, the PLI profile shown by analogue **15** against AChE adopted several key interactions with the active site residues, including the residues Trp70, Trp84, Glu199, Phe331, Tyr334, Trp279 and Tyr70 (Figure 12E), while against the BuChE, this compound adopted several key interactions with Thr120, Asp70, Trp82, His438, Phe329, Trp231, Leu286 and Gly117 (Figure 12F). The elevated potential of this analogue **17** might have been due to the attached electron-withdrawing groups, such as di-Cl and nitro groups on both ends of analogue, where both di-Cl and -NO₂ groups withdraw most of the electronic density from the benzene ring, resulting in a partial positive charge over the benzene ring, and

further this benzene ring tries to re-gain the stability via adopting several key interactions with active side residues, thereby enhancing the enzymatic activity.

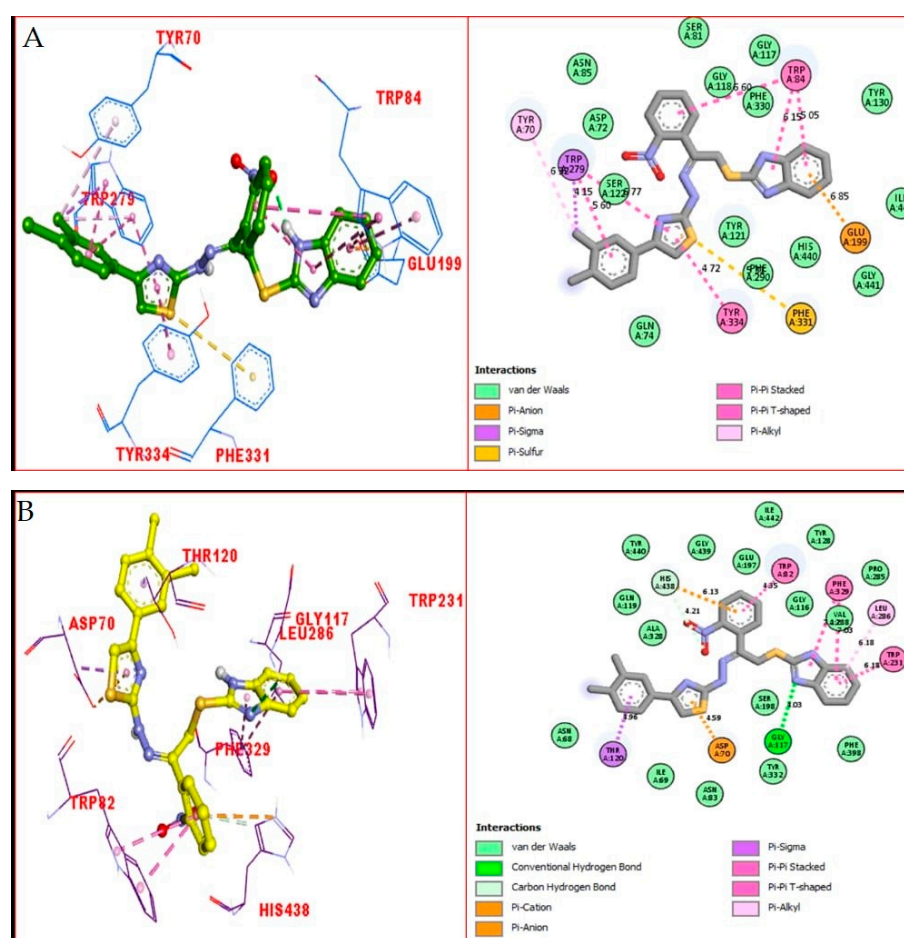


Figure 12. The PLI profile of the third most potent analogue (15):(A) analogue 15 against acetylcholinesterase (AChE);(B) analogue 15 against butyrylcholinesterase (BuChE) enzymes.

The calculated binding energies, number of hydrogen bonds, and number of closest residues surrounding the selected docked analogues into the active sites of both AChE and BuChE enzymes are shown in Table 2.

Table 2. The binding energies, numbers of hydrogen bonds, numbers of closest residues, and the interacting residues of the selected docked analogues into the active sites of both AChE and BuChE.

Active Derivatives	Name of Enzyme	Free Binding Energy (kcal/mol)	Number of HBs	Number of Closest Residues	Interacting Residues
21	AChE	−11.23	1	23	Phe330, Phe331, Tyr334, Asp72, Trp84, Tyr121 and Trp279
	BuChE	−10.88	1	22	Tyr332, Phe329, Ala328, Trp82, Asp70, Gly116, Gly117, Trp231, Ser287 and Leu286
16	AChE	−10.77	1	21	Trp84, Glu199, Tyr121, Trp279, Asp285, Tyr334 and Asp72
	BuChE	−9.89	1	24	Trp231, Leu286, Pro285, Phe329, Asp70, Ile69, Ala328 and Trp82
15	AChE	−9.33	0	20	Trp70, Trp84, Glu199, Phe331, Tyr334, Trp279 and Tyr70
	BuChE	−8.72	1	24	Thr120, Asp70, Trp82, His438, Phe329, Trp231, Leu286 and Gly117

3. Experimental

3.1. General Information

All of the solvents and chemicals, with a purity range of 97 to 99%, were acquired from Sigma Aldrich. Using DMSO as the solvent, the NMR spectra were recorded using a Bruker Ultra Shield Plus NMR spectrometer. By using TMS as reference standard, the chemical shifts values were measured. The high-resolution mass spectra (electron impact, 60 eV) were run on a MAT-311A instrument (Germany). For visualization of the chromatograms, a UV lamp (Schimadzu, Germany) with a wavelength of 254/365 nm was used.

3.2. General Procedure for the Synthesis of Benzimidazole-Bearing 1,3-Thiazole Scaffolds (1–24)

The intermediate (**III**) was obtained by reacting phenacyl bromide (**II**, 1 mmol) with 2-mercapto benzimidazole (**I**, 1 mmol) in EtOH (10 mL) and Et₃N (few drops) and stirred for 2–3 h under reflux condition [44]. An amount of equivalent intermediate (**III**) and thiosemicarbazide were further treated in ethanol (10 mL) and CH₃COOH (glacial) and the solution was refluxed for about 4 h to yield the second intermediate product (**IV**). Finally, intermediate (**IV**) underwent cyclization with stirring overnight with different substituted 2-bromoacetophenone in ethanol (10 mL) Et₃N (few drops) to yield benzimidazole-based thiazole analogues (**1–24**) in moderate to good yield. The solvent was removed after being cooled to room temperature and the resultant solid residue was then cleaned by being washed with n-hexane and re-crystallized from ethyl acetate.

3.3. Spectral Analysis

3.3.1. (E)-4-(2-(2-(2-((1H-benzo[d]imidazol-2-yl)thio)-1-(2-bromophenyl)ethylidene)hydrazinyl)thiazol-4-yl)-2-chloro-5-nitrophenol (**1**)

White crystals. Yield: 68% (0.33 g); ¹H NMR (500 MHz, DMSO-*d*₆): δ 13.25 (s, 1H, -NH), 11.81 (s, -NH, 1H), 10.11 (s, 1H, -OH), 8.28 (s, 1H, H-3''), 8.10 (s, 1H, H-6''), 7.88 (d, $J_{(3',2'/5',6')} = 8.88$ Hz, 2H, H-3'/H-5'), 7.79 (d, $J_{(2',3'/6',5')} = 8.46$ Hz, 2H, H-2'/H-6'), 7.43 (t, $J_{(5(4,6)/6(5,7))} = 7.92$ Hz, 2H, H-5/H-6), 7.27 (d, $J_{(4,5)} = 7.68$ Hz, 1H, H-4), 7.11 (s, 1H, thiazole-H), 7.04 (d, $J_{(7,6)} = 7.56$ Hz, 1H, H-7), 2.34 (s, 2H, S-CH₂); ¹³C-NMR (150 MHz, DMSO-*d*₆): δ 175.8, 143.5, 139.8, 138.9, 137.2, 136.8, 133.6, 132.0, 127.8, 126.2, 125.9, 123.7, 123.5, 123.2, 122.9, 122.9, 122.0, 120.6, 120.6, 119.0, 115.8, 115.3, 110.6, 38.5; HREI-MS: *m/z* [M+H]⁺ calcd for C₂₄H₁₇BrClN₆O₃S₂ 614.9664, found 614.9659. More information, please refer to the Supplementary Materials File.

3.3.2. (E)-4-(2-(2-(2-((1H-benzo[d]imidazol-2-yl)thio)-1-(2-hydroxyphenyl)ethylidene)hydrazinyl)thiazol-4-yl)-2-chloro-5-nitrophenol (**2**)

White crystals. Yield: 64% (0.31 g); ¹H NMR (500 MHz, DMSO-*d*₆): δ 13.39 (s, 1H, -NH), 13.27 (s, 1H, -NH), 12.01 (s, 1H, -OH), 10.15 (s, 1H, -OH), 8.91 (s, 1H, H-3''), 8.30 (s, 1H, H-6''), 8.16–7.87 (m, 4H, H-4/H-5/H-6/H-7), 7.83–7.72 (m, 2H, H-3'/H-6'), 7.45 (t, $J_{(4'/3',5')} = 7.74$ Hz, 1H, H-4'), 7.25 (t, $J_{(5'/4',3')} = 7.74$ Hz, 1H, H-5'), 7.08 (s, 1H, thiazole-H), 2.28 (s, 2H, S-CH₂); ¹³C-NMR (150 MHz, DMSO-*d*₆): δ 183.9, 162.5, 158.4, 157.2, 155.3, 147.4, 146.4, 138.3, 137.2, 135.3, 132.4, 132.1, 131.5, 129.2, 127.5, 127.1, 126.4, 125.5, 124.6, 124.1, 121.0, 118.3, 117.0, 32.0; HREI-MS: *m/z* [M+H]⁺ calcd for C₂₄H₁₈ClN₆O₄S₂ 553.0508, found 553.0502.

3.3.3. (E)-4-(2-(2-(2-((1H-benzo[d]imidazol-2-yl)thio)-1-phenylethylidene)hydrazinyl)thiazol-4-yl)phenol (**3**)

White crystals. Yield: 69% (0.35 g); ¹H NMR (500 MHz, DMSO-*d*₆): δ 12.35 (s, 1H, -NH), 11.78 (s, 1H, -NH), 9.70 (s, 1H, -OH), 7.96 (dd, $J_{(2',3'/6',5')} = 8.1$ Hz, $J_{(2',4'/6',4')} = 2.0$ Hz, 2H, H-2'/H-6'), 7.57–7.49 (m, 3H, H-3'/H-4'/H-5'), 7.43 (d, $J_{(2',3''/6'',5'')} = 7.6$ Hz, 2H, H-2''/H-6''), 6.94 (s, 1H, thiazole-H), 6.91 (d, $J_{(3'',2''/5'',6'')} = 7.8$ Hz, 2H, H-3''/H-5''), 3.56 (s, 2H, S-CH₂); ¹³C-NMR (125 MHz, DMSO-*d*₆): δ 170.8, 157.6, 154.7, 149.3, 146.2, 138.7, 138.0, 133.7, 130.1, 128.0, 128.0, 127.9, 127.9, 127.3, 127.3, 124.7, 122.5, 122.3, 115.5, 115.5,

114.5, 114.3, 104.1, 36.6.; HREI-MS: m/z $[M+H]^+$ calcd for $C_{24}H_{20}N_5O_1S_2$ 458.1106, found 458.1114.

3.3.4. (E)-2-(2-(2-((1H-benzo[d]imidazol-2-yl)thio)-1-phenylethylidene)hydrazinyl)-4-(3-methoxyphenyl)thiazole (4)

Reddish crystals. Yield: 63% (0.30 g); 1H NMR (500 MHz, $DMSO-d_6$): δ 13.25 (s, 1H, -NH), 11.49 (s, 1H, -NH), 7.98 (dd, $J_{(2',3'/6',5')} = 8.4$ Hz, $J_{(2',4'/6',4')} = 2.6$ Hz, 2H, H-2'/H-6'), 7.60–7.55 (m, 3H, H-3'/H-4'/H-5'), 7.53–7.48 (m, 1H, H-6''), 7.41 (t, $J_{(5'',4'',6'')} = 9.6$ Hz, 1H, H-5''), 7.32 (dd, $J_{(2'',6'')} = 2.7$ Hz, $J_{(2'',4'')} = 1.8$ Hz, 1H, H-2''), 7.09 (d, $J_{(4'',5'')} = 8.3$ Hz, 1H, H-4''), 6.95 (s, 1H, thiazole-H), 3.58 (s, 2H, -S-CH₂), 3.84 (s, 3H, -OCH₃); ^{13}C -NMR (125 MHz, $DMSO-d_6$): δ 170.9, 160.3, 154.8, 149.4, 146.3, 138.3, 138.1, 133.2, 133.0, 130.2, 129.4, 128.0, 128.0, 127.4, 127.4, 122.4, 122.2, 119.0, 114.6, 114.4, 113.6, 112.8, 104.2, 55.0, 36.7.; HREI-MS: m/z $[M+H]^+$ calcd for $C_{25}H_{22}N_5O_1S_2$ 472.1263, found 472.1271.

3.3.5. (E)-2-(2-(2-((1H-benzo[d]imidazol-2-yl)thio)-1-phenylethylidene)hydrazinyl)-4-(p-tolyl)thiazole (5)

White crystals. Yield: 60% (0.28 g); 1H NMR (500 MHz, $DMSO-d_6$): δ 13.40 (s, 1H, -NH), 12.87 (s, 1H, -NH), 7.95 (dd, $J_{(2',3'/6',5')} = 7.0$ Hz, $J_{(2',4'/6',4')} = 2.4$ Hz, 2H, H-2'/H-6'), 7.87 (d, $J_{(2'',3''/6'',5'')} = 7.0$ Hz, 2H, H-2''/H-6''), 7.59–7.52 (m, 3H, H-3'/H-4'/H-5'), 7.39 (d, $J_{(3'',2''/5'',6'')} = 6.6$ Hz, 2H, H-3''/H-5''), 6.73 (s, 1H, thiazole-H), 3.49 (s, 2H, -S-CH₂), 2.37 (s, 3H, -CH₃); ^{13}C -NMR (125 MHz, $DMSO-d_6$): δ 171.0, 154.9, 149.5, 146.4, 138.4, 138.2, 133.3, 131.0, 130.3, 129.3, 128.8, 128.8, 128.1, 128.1, 127.5, 127.5, 125.0, 125.0, 122.5, 122.3, 114.7, 114.5, 104.3, 36.8, 20.6.; HREI-MS: m/z $[M+H]^+$ calcd for $C_{25}H_{22}N_5S_2$ 456.1315, found 456.1322.

3.3.6. (E)-2-(2-(2-((1H-benzo[d]imidazol-2-yl)thio)-1-phenylethylidene)hydrazinyl)-4-(3,4-dichlorophenyl)thiazole (6)

White crystals. Yield: 62% (0.28 g); 1H NMR (500 MHz, $DMSO-d_6$): δ 13.39 (s, 1H, -NH), 10.14 (s, 1H, -NH), 7.99 (dd, $J_{(2',3'/6',5')} = 8.7$ Hz, $J_{(2',4'/6',4')} = 2.5$ Hz, 2H, H-2'/H-6'), 7.97 (d, $J_{(2'',6'')} = 2.6$ Hz, 1H, H-2''), 7.82 (dd, $J_{(6'',5'')} = 9.2$ Hz, $J_{(6'',2'')} = 1.9$ Hz, 1H, H-6''), 7.61 (d, $J_{(5'',6'')} = 7.7$ Hz, 1H, H-5''), 7.58–7.53 (m, 3H, H-3'/H-4'/H-5'), 6.86 (s, 1H, thiazole-H), 3.69 (s, 2H, -S-CH₂); ^{13}C -NMR (125 MHz, $DMSO-d_6$): δ 171.2, 155.1, 149.7, 146.6, 138.6, 138.4, 133.5, 132.9, 132.2, 132.0, 130.5, 130.2, 128.5, 128.3, 128.3, 127.7, 127.7, 126.5, 114.9, 122.7, 122.5, 114.7, 104.5, 37.0.; HREI-MS: m/z $[M+H]^+$ calcd for $C_{24}H_{18}Cl_2N_5S_2$ 510.0376, found 510.0386.

3.3.7. (E)-2-(2-(2-((1H-benzo[d]imidazol-2-yl)thio)-1-(p-tolyl)ethylidene)hydrazinyl)-4-(2-nitrophenyl)thiazole (7)

Yellow crystals. Yield: 71% (0.35 g); 1H NMR (500 MHz, $DMSO-d_6$): δ 13.66 (s, 1H, -NH), 10.12 (s, 1H, -NH), 8.10 (dd, $J_{(3',4'')} = 8.0$ Hz, $J_{(3',5'')} = 2.8$ Hz, 1H, H-3''), 8.07 (dd, $J_{(6',5'')} = 7.8$ Hz, $J_{(6',4'')} = 1.6$ Hz, 1H, H-6''), 7.98–7.93 (m, 1H, H-5''), 7.79 (t, $J_{(4'',5'',3'')} = 9.0$ Hz, 1H, H-4''), 7.73 (d, $J_{(2',3'/6',5')} = 7.8$ Hz, 2H, H-2'/H-6'), 7.30 (d, $J_{(3',2'/5',6')} = 8.1$ Hz, 2H, H-3'/H-5'), 6.89 (s, 1H, thiazole-H), 3.70 (s, 2H, -S-CH₂), 2.44 (s, 3H, -CH₃); ^{13}C -NMR (125 MHz, $DMSO-d_6$): δ 171.3, 155.2, 149.8, 148.4, 146.7, 140.3, 138.7, 138.5, 134.9, 132.2, 130.6, 129.2, 128.7, 128.7, 126.6, 126.6, 124.8, 124.0, 122.8, 122.6, 115.0, 114.8, 104.6, 37.1, 20.9.; HREI-MS: m/z $[M+H]^+$ calcd for $C_{25}H_{21}N_6O_2S_2$ 501.1163, found 501.1172.

3.3.8. (E)-2-(2-(2-((1H-benzo[d]imidazol-2-yl)thio)-1-(p-tolyl)ethylidene)hydrazinyl)-4-(3-nitrophenyl)thiazole (8)

White crystals. Yield: 65% (0.32 g); 1H NMR (500 MHz, $DMSO-d_6$): δ 12.42 (s, 1H, -NH), 11.90 (s, 1H, -NH), 8.63 (dd, $J_{(2'',6'')} = 2.5$ Hz, $J_{(2'',4'')} = 1.6$ Hz, 1H, H-2''), 8.35–8.29 (m, 1H, H-6''), 8.26–8.21 (m, 1H, H-4''), 7.87 (t, $J_{(5'',4'',6'')} = 8.8$ Hz, 1H, H-5''), 7.75 (d,

$J_{(2',3'/6',5')} = 7.7$ Hz, 2H, H-2'/H-6'), 7.31 (d, $J_{(3',2'/5',6')} = 8.3$ Hz, 2H, H-3'/H-5'), 6.87 (s, 1H, thiazole-H), 3.69 (s, 2H, -S-CH₂), 2.42 (s, 3H, -CH₃); ¹³C-NMR (125 MHz, DMSO-d₆): δ 171.4, 155.3, 149.9, 148.1, 146.8, 140.4, 138.8, 138.6, 133.6, 133.3, 130.7, 130.3, 128.8, 128.8, 126.7, 126.7, 123.6, 122.9, 122.7, 122.4, 115.1, 114.9, 104.7, 37.2, 21.0.; HREI-MS: *m/z* [M+H]⁺ calcd for C₂₅H₂₁N₆O₂S₂ 501.1163, found 501.1172.

3.3.9. (E)-4-(2-(2-(2-((1H-benzo[d]imidazol-2-yl)thio)-1-(3-hydroxy-2-nitrophenyl)ethylidene)hydrazinyl)thiazol-4-yl)-2-chloro-5-nitrophenol (**9**)

Yellow crystals. Yield: 73% (0.37 g); ¹H NMR (500 MHz, DMSO-*d*₆): δ 13.39 (s, 1H, -NH), 13.30 (s, 1H, -NH), 12.21 (s, 1H, -OH), 10.51 (s, 1H, -OH), 8.91 (s, 1H, H-3''), 8.35 (s, 1H, H-6''), 8.30 (d, $J_{(6'/5')} = 9.62$ Hz, 1H, H-6'), 8.27–8.03 (m, 1H, H-4'), 7.91–7.85 (m, 1H, H-5'), 7.83 (d, $J_{(4,5/7,6)} = 9.0$ Hz, 2H, H-4/H-7), 7.76 (t, $J_{(5(4,6)/6(5,7))} = 8.52$ Hz, 2H, H-5/H-6), 7.10 (s, 1H, thiazole-H), 2.34 (s, 2H, S-CH₂); ¹³C-NMR (150 MHz, DMSO-d₆): δ 175.2, 162.1, 155.6, 143.1, 135.5, 135.6, 133.7, 131.7, 127.6, 127.3, 126.4, 126.3, 124.4, 123.8, 123.7, 121.0, 120.9, 120.7, 119.0, 118.8, 117.9, 112.4, 112.3, 30.4.; HREI-MS: *m/z* [M+H]⁺ calcd for C₂₄H₁₇ClN₇O₆S₂ 598.0365, found 598.0358.

3.3.10. (E)-5-(2-(2-(2-((1H-benzo[d]imidazol-2-yl)thio)-1-([1,1'-biphenyl]-4-yl)ethylidene)hydrazinyl)thiazol-4-yl)-2-(dimethylamino)-4-nitrophenol (**10**)

White crystals. Yield: 60% (0.29 g); ¹H NMR (500 MHz, DMSO-*d*₆): δ 13.64 (s, 1H, -NH), 11.54 (s, 1H, -NH), 10.12 (s, 1H, -OH), 8.23 (s, 1H, H-3''), 8.18 (s, 1H, H-6''), 8.04 (d, $J_{(3,2/5,6)} = 7.26$ Hz, 4H, H-4/H-5/H-6/H-7), 7.99–7.92 (m, 4H, H-2'/H-3'/H-5'/H-6'), 7.64–7.59 (m, 5H, Ph-H), 7.03 (s, 1H, thiazole-H), 4.03 (s, 6H, -CH₃), 2.51 (s, 2H, S-CH₂); ¹³C-NMR (150 MHz, DMSO-d₆): δ 188.5, 158.5, 157.3, 155.2, 148.3, 147.7, 143.0, 140.6, 139.4, 134.1, 133.8, 133.8, 130.0, 129.0, 128.9, 128.9, 127.9, 125.9, 125.9, 123.4, 121.3, 121.3, 120.6, 119.1, 119.1, 118.4, 118.4, 115.9, 115.2, 40.5, 40.5, 31.4.; HREI-MS: *m/z* [M+H]⁺ calcd for C₃₂H₂₈N₇O₃S₂ 622.1683, found 622.1678.

3.3.11. (E)-2-(2-(2-((1H-benzo[d]imidazol-2-yl)thio)-1-(p-tolyl)ethylidene)hydrazinyl)-4-(3,4-dichlorophenyl)thiazole (**11**)

White crystals. Yield: 70% (0.34 g); ¹H NMR (500 MHz, DMSO-*d*₆): δ 12.53 (s, 1H, -NH), 11.69 (s, 1H, -NH), 7.97 (d, $J_{(2'',6'')} = 2.5$ Hz, 1H, H-2''), 7.83 (dd, $J_{(6'',5'')} = 9.5$ Hz, $J_{(6'',2'')} = 1.9$ Hz, 1H, H-6''), 7.79 (d, $J_{(2',3'/6',5')} = 8.5$ Hz, 2H, H-2'/H-6'), 7.62 (d, $J_{(5'',6'')} = 7.8$ Hz, 1H, H-5''), 7.38 (d, $J_{(3',2'/5',6')} = 8.6$ Hz, 2H, H-3'/H-5'), 6.89 (s, 1H, thiazole-H), 3.58 (s, 2H, -S-CH₂), 2.43 (s, 3H, -CH₃); ¹³C-NMR (125 MHz, DMSO-d₆): δ 171.8, 155.7, 150.3, 147.2, 140.8, 139.0, 138.8, 133.5, 132.8, 132.6, 131.1, 130.8, 129.2, 129.2, 128.9, 127.3, 127.1, 127.1, 123.1, 122.9, 115.3, 115.1, 105.1, 37.6, 21.4.; HREI-MS: *m/z* [M+H]⁺ calcd for C₂₅H₂₀Cl₂N₅S₂ 524.0533, found 524.0542.

3.3.12. (E)-4-(2-(2-(2-((1H-benzo[d]imidazol-2-yl)thio)-1-(4-methyl-2-nitrophenyl)ethylidene)hydrazinyl)thiazol-4-yl)-2-chloro-5-nitrophenol (**12**)

White crystals. Yield: 62% (0.30 g); ¹H NMR (500 MHz, DMSO-*d*₆): δ 13.62 (s, 1H, NH), 13.38 (s, 1H, NH), 10.12 (s, 1H, -OH), 8.90 (s, 1H, H-3''), 8.23 (s, 1H, H-6''), 8.16 (s, 1H, H-3'), 8.02 (d, $J_{(5',6')} = 5.58$ Hz, 1H, H-5'), 7.87 (d, $J_{(6',5')} = 8.46$ Hz, 1H, H-6'), 7.75 (d, $J_{(3,2/5,6)} = 8.4$ Hz, 2H, H-4/H-7), 7.61 (t, $J_{(5(4,6)/6(5,7))} = 8.34$ Hz, 2H, H-5/H-6), 6.98 (s, 1H, thiazole-H), 2.50 (s, 2H, S-CH₂), 1.91 (s, 3H, -CH₃); ¹³C-NMR (150 MHz, DMSO-d₆): δ 183.5, 162.1, 157.4, 155.3, 147.5, 147.2, 146.5, 141.4, 139.8, 137.0, 135.1, 133.8, 131.8, 129.9, 129.0, 126.8, 126.5, 125.4, 125.2, 124.4, 121.0, 118.8, 112.3, 30.5, 20.0.; HREI-MS: *m/z* [M+H]⁺ calcd for C₂₅H₁₉ClN₇O₅S₂ 596.0567, found 596.0561.

3.3.13. (E)-2-(2-(2-((1H-benzo[d]imidazol-2-yl)thio)-1-(2-nitrophenyl)ethylidene)hydrazinyl)-4-(p-tolyl)thiazole (13)

White microcrystals. Yield: 59% (0.27 g); ^1H NMR (500 MHz, $\text{DMSO-}d_6$): δ 13.40 (s, 1H, -NH), 10.95 (s, 1H, -NH), 8.15 (dd, $J_{(6',5')} = 6.7$ Hz, $J_{(6',4')} = 2.5$ Hz, 1H, H-6'), 8.04 (dd, $J_{(3',4')} = 6.9$ Hz, $J_{(3',5')} = 1.6$ Hz, 1H, H-3'), 7.93–7.89 (m, 1H, H-5'), 7.84 (d, $J_{(2'',3''/6'',5'')} = 8.0$ Hz, 2H, H-2''/H-6''), 7.66 (t, $J_{(4'/5',3')} = 9.2$ Hz, 1H, H-4'), 7.40 (d, $J_{(3'',2''/5'',6'')} = 7.2$ Hz, 2H, H-3''/H-5''), 6.97 (s, 1H, thiazole-H), 3.71 (s, 2H, -S-CH₂), 2.34 (s, 3H, -CH₃); ^{13}C -NMR (125 MHz, $\text{DMSO-}d_6$): δ 172.0, 155.9, 150.5, 147.4, 139.2, 139.0, 135.7, 134.6, 132.5, 132.2, 132.0, 130.3, 129.8, 129.8, 126.7, 126.0, 126.0, 125.7, 123.3, 123.1, 115.5, 115.3, 105.3, 37.8, 21.6.; HREI-MS: m/z $[\text{M}+\text{H}]^+$ calcd for $\text{C}_{25}\text{H}_{21}\text{N}_6\text{O}_2\text{S}_2$ 501.1163, found 501.1172.

3.3.14. (E)-2-(2-(2-((1H-benzo[d]imidazol-2-yl)thio)-1-(2-nitrophenyl)ethylidene)hydrazinyl)-4-(3-methoxyphenyl)thiazole (14)

White crystals. Yield: 58% (0.26 g); ^1H NMR (500 MHz, $\text{DMSO-}d_6$): δ 12.61 (s, 1H, -NH), 12.01 (s, 1H, -NH), 8.17 (dd, $J_{(6',5')} = 6.5$ Hz, $J_{(6',4')} = 2.5$ Hz, 1H, H-6'), 8.08 (dd, $J_{(3',4')} = 6.8$ Hz, $J_{(3',5')} = 1.8$ Hz, 1H, H-3'), 7.84–7.78 (m, 1H, H-5'), 7.68 (t, $J_{(4'/5',3')} = 8.2$ Hz, 1H, H-4'), 7.58–7.53 (m, 1H, H-6''), 7.46 (t, $J_{(5''/4'',6'')} = 9.8$ Hz, 1H, H-5''), 7.35 (dd, $J_{(2'',6'')} = 2.0$ Hz, $J_{(2'',4'')} = 2.4$ Hz, 1H, H-2''), 7.12 (d, $J_{(4'',5'')} = 8.3$ Hz, 1H, H-4''), 7.02 (s, 1H, thiazole-H), 3.86 (s, 3H, -OCH₃), 3.80 (s, 2H, -S-CH₂); ^{13}C -NMR (125 MHz, $\text{DMSO-}d_6$): δ 171.9, 161.3, 155.8, 150.4, 147.3, 139.1, 138.9, 135.6, 134.5, 134.2, 132.2, 132.0, 130.4, 126.6, 125.6, 123.2, 123.0, 120.0, 115.4, 115.2, 114.5, 113.8, 105.2, 56.0, 37.7.; HREI-MS: m/z $[\text{M}+\text{H}]^+$ calcd for $\text{C}_{25}\text{H}_{21}\text{N}_6\text{O}_3\text{S}_2$ 517.1113, found 517.1123.

3.3.15. (E)-2-(2-(2-((1H-benzo[d]imidazol-2-yl)thio)-1-(2-nitrophenyl)ethylidene)hydrazinyl)-4-(3,4-dichlorophenyl)thiazole (15)

White microcrystals. Yield: 63% (0.33 g); ^1H NMR (500 MHz, $\text{DMSO-}d_6$): δ 12.61 (s, 1H, -NH), 12.01 (s, 1H, -NH), 8.20 (dd, $J_{(6',5')} = 7.0$ Hz, $J_{(6',4')} = 2.3$ Hz, 1H, H-6'), 8.13 (dd, $J_{(3',4')} = 7.4$ Hz, $J_{(3',5')} = 2.6$ Hz, 1H, H-3'), 8.01 (d, $J_{(2'',6'')} = 1.6$ Hz, 1H, H-2''), 7.97–7.92 (m, 1H, H-5'), 7.85 (dd, $J_{(6'',5'')} = 8.6$ Hz, $J_{(6'',2'')} = 1.7$ Hz, 1H, H-6''), 7.69 (t, $J_{(4'/5',3')} = 9.5$ Hz, 1H, H-4'), 7.64 (d, $J_{(5''/6'')} = 7.7$ Hz, 1H, H-5''), 7.02 (s, 1H, thiazole-H), 3.80 (s, 2H, -S-CH₂); ^{13}C -NMR (125 MHz, $\text{DMSO-}d_6$): δ 172.6, 156.5, 151.1, 148.0, 139.8, 139.6, 135.3, 135.1, 134.3, 133.6, 133.4, 132.7, 132.5, 131.6, 129.7, 127.9, 127.5, 126.3, 123.9, 123.7, 116.1, 115.9, 105.9, 38.4.; HREI-MS: m/z $[\text{M}+\text{H}]^+$ calcd for $\text{C}_{24}\text{H}_{17}\text{Cl}_2\text{N}_6\text{O}_2\text{S}_2$ 555.0227, found 555.0236.

3.3.16. (E)-4-(2-(2-(2-((1H-benzo[d]imidazol-2-yl)thio)-1-(2-nitrophenyl)ethylidene)hydrazinyl)thiazol-4-yl)phenol (16)

White microcrystals. Yield: 62% (0.32 g); ^1H NMR (500 MHz, $\text{DMSO-}d_6$): δ 12.39 (s, 1H, -NH), 11.88 (s, 1H, -NH), 9.72 (s, 1H, -OH), 8.12 (dd, $J_{(6',5')} = 7.6$ Hz, $J_{(6',4')} = 2.6$ Hz, 1H, H-6'), 8.05 (dd, $J_{(3',4')} = 7.9$ Hz, $J_{(3',5')} = 1.9$ Hz, 1H, H-3'), 7.79–7.74 (m, 1H, H-5'), 7.65 (t, $J_{(4'/5',3')} = 9.2$ Hz, 1H, H-4'), 7.42 (d, $J_{(2'',3''/6'',5'')} = 7.2$ Hz, 2H, H-2''/H-6''), 6.93 (d, $J_{(3'',2''/5'',6'')} = 7.7$ Hz, 2H, H-3''/H-5''), 6.75 (s, 1H, thiazole-H), 3.58 (s, 2H, -S-CH₂); ^{13}C -NMR (125 MHz, $\text{DMSO-}d_6$): δ 172.1, 158.9, 156.0, 150.6, 147.5, 139.3, 139.1, 134.8, 134.6, 132.2, 132.0, 129.3, 129.3, 126.8, 126.0, 125.8, 123.4, 123.2, 116.8, 116.8, 115.6, 115.4, 105.4, 37.9.; HREI-MS: m/z $[\text{M}+\text{H}]^+$ calcd for $\text{C}_{24}\text{H}_{19}\text{N}_6\text{O}_3\text{S}_2$ 503.0958, found 503.0965.

3.3.17. (E)-2-(2-(2-((1H-benzo[d]imidazol-2-yl)thio)-1-(3,4-dichlorophenyl)ethylidene)hydrazinyl)-4-(2-nitrophenyl)thiazole (17)

White microcrystals. Yield: 64% (0.33 g); ^1H NMR (500 MHz, $\text{DMSO-}d_6$): δ 12.62 (s, 1H, -NH), 12.03 (s, 1H, -NH), 8.13 (dd, $J_{(6',5')} = 8.2$ Hz, $J_{(6',4')} = 2.5$ Hz, 1H, H-6''), 8.06 (dd, $J_{(3',4')} = 8.8$ Hz, $J_{(3',5')} = 2.2$ Hz, 1H, H-3''), 7.97–7.93 (m, 1H, H-5''), 7.89 (d, $J_{(2',6')} = 2.3$ Hz, 1H, H-2'), 7.85 (dd, $J_{(6',5')} = 8.4$ Hz, $J_{(6',2')} = 1.8$ Hz, 1H, H-6'), 7.81 (t, $J_{(4'/5',3')} = 9.5$ Hz, 1H, H-4''), 7.73 (d, $J_{(5',6')} = 7.6$ Hz, 1H, H-5'), 7.06 (s, 1H, thiazole-H), 3.81 (s, 2H, -S-CH₂); ^{13}C -NMR (125 MHz, $\text{DMSO-}d_6$): δ 172.5, 156.4, 151.0, 149.2, 147.9, 139.7, 139.5, 136.5, 136.3,

136.1, 134.3, 133.4, 131.4, 131.1, 130.4, 127.1, 126.0, 125.2, 123.8, 123.6, 116.0, 115.8, 105.8, 38.3.; HREI-MS: m/z $[M+H]^+$ calcd for $C_{24}H_{17}Cl_2N_6O_2S_2$ 555.0227, found 555.0236.

3.3.18. (E)-2-(2-(2-((1H-benzo[d]imidazol-2-yl)thio)-1-(3,4-dichlorophenyl)ethylidene)hydrazinyl)-4-(3-nitrophenyl)thiazole (18)

Reddish microcrystals. Yield: 61% (0.30 g); 1H NMR (500 MHz, DMSO- d_6): δ 12.66 (s, 1H, -NH), 12.09 (s, 1H, -NH), 8.61 (dd, $J_{(2'',6'')} = 2.0$ Hz, $J_{(2'',4'')} = 2.2$ Hz, 1H, H-2''), 8.32–8.27 (m, 1H, H-6''), 8.21–8.14 (m, 1H, H-4''), 7.95 (d, $J_{(2',6')} = 2.5$ Hz, 1H, H-2'), 7.89 (t, $J_{(5''/4'',6'')} = 9.0$ Hz, 1H, H-5''), 7.85 (dd, $J_{(6',5')} = 8.7$ Hz, $J_{(6',2')} = 1.4$ Hz, 1H, H-6'), 7.76 (d, $J_{(5',6')} = 7.8$ Hz, 1H, H-5'), 7.10 (s, 1H, thiazole-H), 3.83 (s, 2H, -S-CH₂); ^{13}C -NMR (125 MHz, DMSO- d_6): δ 172.3, 156.2, 150.8, 149.0, 147.7, 139.5, 139.3, 136.3, 136.1, 134.5, 134.3, 134.1, 132.2, 131.2, 130.9, 126.9, 124.4, 123.6, 123.4, 123.2, 115.8, 115.6, 105.6, 38.1.; HREI-MS: m/z $[M+H]^+$ calcd for $C_{24}H_{17}Cl_2N_6O_2S_2$ 555.0227, found 555.0236.

3.3.19. (E)-2-(2-(2-((1H-benzo[d]imidazol-2-yl)thio)-1-(3,4-dichlorophenyl)ethylidene)hydrazinyl)-4-(p-tolyl)thiazole (19)

Yellow crystals. Yield: 65% (0.36 g); 1H NMR (500 MHz, DMSO- d_6): δ 12.59 (s, 1H, -NH), 11.97 (s, 1H, -NH), 7.97 (d, $J_{(2',6')} = 2.0$ Hz, 1H, H-2'), 7.87 (dd, $J_{(6',5')} = 8.5$ Hz, $J_{(6',2')} = 1.5$ Hz, 1H, H-6'), 7.83 (d, $J_{(2'',3''/6'',5'')} = 7.8$ Hz, 2H, H-2''/H-6''), 7.70 (d, $J_{(5',6')} = 0.9$ Hz, 1H, H-5'), 7.42 (d, $J_{(3'',2''/5'',6'')} = 8.4$ Hz, 2H, H-3''/H-5''), 6.99 (s, 1H, thiazole-H), 3.67 (s, 2H, -S-CH₂), 2.41 (s, 3H, -CH₃); ^{13}C -NMR (125 MHz, DMSO- d_6): δ 171.8, 155.7, 150.3, 147.2, 139.0, 138.8, 135.8, 135.6, 133.6, 131.9, 130.7, 130.4, 130.2, 129.7, 129.7, 126.4, 125.9, 125.9, 123.1, 122.9, 115.3, 115.1, 105.1, 37.6, 21.6.; HREI-MS: m/z $[M+H]^+$ calcd for $C_{25}H_{20}Cl_2N_5S_2$ 524.0533, found 524.0542.

3.3.20. (E)-2-(2-(2-((1H-benzo[d]imidazol-2-yl)thio)-1-(3,4-dichlorophenyl)ethylidene)hydrazinyl)-4-(3-methoxyphenyl)thiazole (20)

Reddish microcrystals. Yield: 61% (0.31 g); 1H NMR (500 MHz, DMSO- d_6): δ 12.62 (s, 1H, -NH), 11.99 (s, 1H, -NH), 7.98 (d, $J_{(2',6')} = 1.7$ Hz, 1H, H-2'), 7.84 (dd, $J_{(6',5')} = 8.6$ Hz, $J_{(6',2')} = 2.3$ Hz, 1H, H-6'), 7.69 (d, $J_{(5',6')} = 7.5$ Hz, 1H, H-5'), 7.54–7.47 (m, 1H, H-6''), 7.40 (t, $J_{(5''/4'',6'')} = 9.0$ Hz, 1H, H-5''), 7.29 (dd, $J_{(2'',6'')} = 2.9$ Hz, $J_{(2'',4'')} = 1.4$ Hz, 1H, H-2''), 7.06 (d, $J_{(4'',5'')} = 8.5$ Hz, 1H, H-4''), 7.02 (s, 1H, thiazole-H), 3.83 (s, 3H, -OCH₃), 3.78 (s, 2H, -S-CH₂); ^{13}C -NMR (125 MHz, DMSO- d_6): δ 172.4, 161.8, 156.3, 150.9, 147.8, 139.6, 139.4, 136.4, 135.2, 134.7, 134.2, 131.3, 131.0, 130.9, 127.0, 123.7, 123.5, 120.5, 115.9, 115.7, 115.0, 114.3, 105.7, 56.5, 38.2.; HREI-MS: m/z $[M+H]^+$ calcd for $C_{25}H_{20}Cl_2N_5OS_2$ 540.0483, found 540.0491.

3.3.21. (E)-2-(2-(2-((1H-benzo[d]imidazol-2-yl)thio)-1-(3,4-dichlorophenyl)ethylidene)hydrazinyl)-4-(3,4-dichlorophenyl)thiazole (21)

Reddish microcrystals. Yield: 63% (0.34 g); 1H NMR (500 MHz, DMSO- d_6): δ 12.65 (s, 1H, -NH), 12.11 (s, 1H, -NH), 8.03 (d, $J_{(2'',6'')} = 2.8$ Hz, 1H, H-2''), 7.94 (d, $J_{(2',6')} = 2.4$ Hz, 1H, H-2'), 7.88 (dd, $J_{(6'',5'')} = 9.0$ Hz, $J_{(6'',2'')} = 1.5$ Hz, 1H, H-6''), 7.84 (dd, $J_{(6',5')} = 8.8$ Hz, $J_{(6',2')} = 2.6$ Hz, 1H, H-6'), 7.74 (d, $J_{(5',6')} = 7.0$ Hz, 1H, H-5'), 7.59 (d, $J_{(5'',6'')} = 7.3$ Hz, 1H, H-5''), 7.08 (s, 1H, thiazole-H), 3.86 (s, 2H, -S-CH₂); ^{13}C -NMR (125 MHz, DMSO- d_6): δ 172.2, 156.1, 150.7, 147.6, 139.4, 139.2, 136.2, 136.0, 134.0, 133.9, 133.2, 133.0, 131.3, 131.1, 130.8, 129.3, 127.5, 126.8, 123.5, 123.3, 115.7, 115.5, 105.5, 38.0.; HREI-MS: m/z $[M+H]^+$ calcd for $C_{24}H_{16}Cl_4N_5S_2$ 579.9568, found 579.9577.

3.3.22. (E)-2-(2-(2-((1H-benzo[d]imidazol-2-yl)thio)-1-(3,4-dichlorophenyl)ethylidene)hydrazinyl)-4-(2-methoxyphenyl)thiazole (22)

White microcrystals. Yield: 68% (0.37 g); 1H NMR (500 MHz, DMSO- d_6): δ 12.49 (s, 1H, -NH), 11.69 (s, 1H, -NH), 8.43 (dd, $J_{(6'',5'')} = 7.6$ Hz, $J_{(6'',4'')} = 1.9$ Hz, 1H, H-6''), 7.91 (d, $J_{(2',6')} = 2.9$ Hz, 1H, H-2'), 7.82 (dd, $J_{(6',5')} = 7.5$ Hz, $J_{(6',2')} = 2.1$ Hz, 1H, H-6'), 7.78 (d, $J_{(5',6')} = 7.8$ Hz, 1H, H-5'), 7.52 (t, $J_{(4''/5'',3'')} = 9.4$ Hz, 1H, H-4''), 7.43–7.37 (m, 1H, H-5''), 7.18 (dd, $J_{(3'',4'')} = 8.5$ Hz, $J_{(3'',5'')} = 1.5$ Hz, 1H, H-3''), 7.03 (s, 1H, thiazole-H), 3.82 (s, 3H, -CH₃),

3.59 (s, 2H, -S-CH₂); ¹³C-NMR (125 MHz, DMSO-d₆): δ 171.9, 157.5, 155.8, 150.4, 147.3, 139.1, 138.9, 135.9, 135.7, 133.7, 131.3, 130.8, 130.5, 129.9, 126.5, 123.2, 123.0, 121.7, 119.1, 115.4, 115.2, 111.3, 105.2, 56.3, 37.7.; HREI-MS: m/z [M+H]⁺ calcd for C₂₅H₂₀Cl₂N₅OS₂ 540.0483, found 540.0491.

3.3.23. (E)-2-(2-(2-((1H-benzo[d]imidazol-2-yl)thio)-1-(3,4-dichlorophenyl)ethylidene)hydrazinyl)-4-(4-bromophenyl)thiazole (23)

Reddish microcrystals. Yield: 60% (0.29 g); ¹H NMR (500 MHz, DMSO-d₆): δ 12.44 (s, 1H, -NH), 11.73 (s, 1H, -NH), 7.93 (d, *J*_(2',6') = 2.8 Hz, 1H, H-2'), 7.87 (dd, *J*_(6',5') = 8.5 Hz, *J*_(6',2') = 1.7 Hz, 1H, H-6'), 7.79 (d, *J*_(2'',3''/6'',5'') = 7.4 Hz, 2H, H-2''/H-6''), 7.72 (d, *J*_(5',6') = 7.7 Hz, 1H, H-5'), 7.58 (d, *J*_(3'',2''/5'',6'') = 6.9 Hz, 2H, H-3''/H-5''), 6.88 (s, 1H, thiazole-H), 3.48 (s, 2H, -S-CH₂); ¹³C-NMR (125 MHz, DMSO-d₆): δ 171.5, 155.4, 150.0, 146.9, 138.7, 138.5, 135.5, 135.3, 133.3, 131.9, 131.9, 131.7, 130.4, 130.1, 128.1, 128.1, 126.1, 122.9, 122.7, 122.6, 115.0, 114.8, 104.2, 37.3.; HREI-MS: m/z [M+H]⁺ calcd for C₂₄H₁₇BrCl₂N₅S₂ 587.9484, found 587.9491.

3.3.24. (E)-2-(2-(2-((1H-benzo[d]imidazol-2-yl)thio)-1-(p-tolyl)ethylidene)hydrazinyl)-4-(p-tolyl)thiazole (24)

Yellow crystals. Yield: 73% (0.37 g); ¹H NMR (500 MHz, DMSO-d₆): δ 12.45 (s, 1H, -NH), 11.78 (s, 1H, -NH), 7.86 (d, *J*_(2'',3''/6'',5'') = 7.5 Hz, 2H, H-2''/H-6''), 7.72 (d, *J*_(2',3'/6',5') = 6.8 Hz, 2H, H-2'/H-6'), 7.37 (d, *J*_(3'',2''/5'',6'') = 6.8 Hz, 2H, H-3''/H-5''), 7.34 (d, *J*_(3',2'/5',6') = 6.9 Hz, 2H, H-3'/H-5'), 6.77 (s, 1H, thiazole-H), 3.56 (s, 2H, -S-CH₂), 2.46 (s, 3H, -CH₃), 2.38 (s, 3H, -CH₃); ¹³C-NMR (125 MHz, DMSO-d₆): δ 171.1, 155.9, 149.5, 146.5, 140.2, 138.5, 138.3, 131.1, 130.4, 129.3, 128.8, 128.8, 128.5, 128.5, 126.4, 126.4, 125.1, 125.1, 122.6, 122.4, 114.8, 114.6, 104.4, 36.9, 20.5, 20.6.; HREI-MS: m/z [M+H]⁺ calcd for C₂₆H₂₄N₅S₂ 470.1469, found 470.1478.

3.4. Molecular Docking Protocol

The MOE software programme was used in molecular docking to determine how synthesized analogues interact with both targeted enzyme (AChE & BuChE) to triangulate the outcomes from in vitro and in silico analysis. Using the PDB codes 1ACL for AChE and 1POP for BuChE, the RCSB protein databank's crystal structures for both targets were retrieved. The crystallographic structures and all synthesized analogues were protonated using the default MOE-Dock module parameters, resulting in analogue structures and optimized enzyme. After this, a docking study was conducted using the optimized enzyme and analogues structures. Our earlier investigations contain all of the detailed information about the docking process [47–49].

3.5. Acetylcholinesterase Activity Assay Protocol

The inhibition of AChE and BChE was determined using a method described earlier [50,51]. Briefly, the stock solutions (1 mg/mL) of test analogues were prepared using DMSO. The working solutions (1–100 µg/mL) were prepared using serial dilutions (a serial dilution means a series of diluted solutions, e.g., 0.1 mg/mL, 0.2 mg/mL and so on; the solutions contained 5% DMSO and 95% water). The various concentrations of test compounds (10 µL) were pre-incubated with sodium phosphate buffer (0.1 M; pH 8.0; 150 µL) and AChE (0.1 U/mL; 20 µL) for 15 min at 25 °C. The reaction was initiated via the addition of DTNB (1 mM; 10 µL) and AChEI (1 mM; 10 µL). The mixture of reaction was mixed using a cyclomixer and incubated for 10 min at 25 °C. The absorbance was measured using a microplate reader at a 410 nm wavelength against the blank reading containing 10 µL DMSO instead of the test compound (the solution contained 5% DMSO and 95% water). Utilizing the formula given in Equation (1), the percentage of inhibition was computed, and the IC₅₀ was determined under the positive control of Donepezil (0.01–100 g/mL).

$$\% \text{ Inhibition} = (\text{Absorbance of control} - \text{Absorbance of compound}) / \text{Absorbance of control} \times 100$$

IC₅₀ is the concentration of a drug or inhibitor required to inhibit 50% of an enzyme's activity which was calculated by constructing a non-linear regression graph between

the percentages of inhibition vs. concentration, using Graph Pad prism software (version 5.3)(accessed on 5 August 2022).

4. Conclusions

All of the newly synthesized derivatives of benzimidazole-based thiazole (**1–24**) were evaluated for inhibitory potentials (in vitro) against AChE and BuChE enzymes, respectively. Moreover, all derivatives (except derivative **10** due to its inactivity) displayed moderate to good inhibitory potentials in the range of 0.10 ± 0.05 to 11.10 ± 0.30 μM (for AChE) and 0.20 ± 0.050 μM to 14.20 ± 0.10 μM (for BuChE) under the positive control of Donepezil ($\text{IC}_{50} = 2.16 \pm 0.12$ μM (for AChE) and 4.5 ± 0.11 μM (for BuChE)). Among the synthesized series, the analogue **21** ($\text{IC}_{50} = 0.10$ μM (for AChE) and 0.20 μM (for BuChE)) was identified as the most effective inhibitor of AChE and BuChE, even more potent than the standard, Donepezil.

Supplementary Materials: The following supporting information can be downloaded at: <https://www.mdpi.com/article/10.3390/molecules27186087/s1>, Figure-S1:Protein Ligand interaction (PLI) profile of compounds **24** against acetylcholinesterase (AChE); Figure-S2:Protein Ligand interaction (PLI) profile of compounds **24** against butyrylcholinesterase (BuChE); Figure-S3:Protein Ligand interaction (PLI) profile of compounds **7** against acetylcholinesterase (AChE); Figure-S4:Protein Ligand interaction (PLI) profile of compounds **7** against butyrylcholinesterase (BuChE); Figure-S5: $^1\text{H-NMR}$ of (*E*)-4-(2-(2-(2-((1*H*-benzo[d]imidazol-2-yl)thio)-1-(2-bromophenyl)ethylidene)hydrazinyl)thiazol-4-yl)-2-chloro-5-nitrophenol (**1**); Figure-S6: $^{13}\text{C-NMR}$ of (*E*)-4-(2-(2-(2-((1*H*-benzo[d]imidazol-2-yl)thio)-1-(2-bromophenyl)ethylidene)hydrazinyl)thiazol-4-yl)-2-chloro-5-nitrophenol (**1**); Figure-S7: $^1\text{H-NMR}$ of (*E*)-4-(2-(2-(2-((1*H*-benzo[d]imidazol-2-yl)thio)-1-(2-hydroxyphenyl)ethylidene)hydrazinyl)thiazol-4-yl)-2-chloro-5-nitrophenol (**2**); Figure-S8: $^1\text{H-NMR}$ of (*E*)-4-(2-(2-(2-((1*H*-benzo[d]imidazol-2-yl)thio)-1-(3-hydroxy-2nitrophenyl)ethylidene)hydrazinyl)thiazol-4-yl)-2-chloro-5-nitrophenol (**9**); Figure-S9: $^{13}\text{C-NMR}$ of (*E*)-4-(2-(2-(2-((1*H*-benzo[d]imidazol-2-yl)thio)-1-(3-hydroxy-2nitrophenyl)ethylidene)hydrazinyl)thiazol-4-yl)-2-chloro-5-nitrophenol (**9**); Figure-S10: $^1\text{H-NMR}$ (*E*)-5-(2-(2-(2-((1*H*-benzo[d]imidazol-2-yl)thio)-1-([1,1'-biphenyl]-4yl)ethylidene)hydrazinyl)thiazol-4-yl)-2-(dimethylamino)-4-nitrophenol (**10**); Figure-S11: $^{13}\text{C-NMR}$ (*E*)-5-(2-(2-(2-((1*H*-benzo[d]imidazol-2-yl)thio)-1-([1,1'-biphenyl]-4yl)ethylidene)hydrazinyl)thiazol-4-yl)-2-(dimethylamino)-4-nitrophenol (**10**); Figure-S12: $^1\text{H-NMR}$ of (*E*)-4-(2-(2-(2-((1*H*-benzo[d]imidazol-2-yl)thio)-1-(4-methyl-2nitrophenyl)ethylidene)hydrazinyl)thiazol-4-yl)-2-chloro-5-nitrophenol (**12**); Figure-S13: $^{13}\text{C-NMR}$ of (*E*)-4-(2-(2-(2-((1*H*-benzo[d]imidazol-2-yl)thio)-1-(4-methyl-2nitrophenyl)ethylidene)hydrazinyl)thiazol-4-yl)-2-chloro-5-nitrophenol (**12**).

Author Contributions: Conceptualization, H.U. and F.R.; methodology, R.H.; software, S.K.; validation, M.A., A.S.A. and O.A.; formal analysis, S.A.A.S. and M.T.; investigation, M.T.; resources, M.T. and F.R.; data curation, M.A.A.; writing—original draft preparation, H.U. and F.R.; writing—review and editing, R.I., M.S. and W.R.; visualization, M.S. and S.H.; supervision, F.R.; project administration, F.R. and H.U.; funding acquisition, M.A., A.S.A., M.A.A. and O.A. All authors have read and agreed to the published version of the manuscript.

Funding: The current works supporting by Taif University Researchers Supporting Project number (TURSP-2020/257), Taif University, Taif, Saudi Arabia.

Institutional Review Board Statement: Not applicable.

Informed Consent Statement: Not applicable.

Data Availability Statement: Not applicable.

Acknowledgments: The authors extend their appreciation to Taif University for supporting the current work by Taif University Researchers Supporting Project number (TURSP-2020/257), Taif University, Taif, Saudi Arabia.

Conflicts of Interest: All the authors have declared that they have no conflict of interest.

References

1. Ahmad, S.; Iftikhar, F.; Ullah, F.; Sadiq, A.; Rashid, U. Rational design and synthesis of dihydropyrimidine based dual binding site acetylcholinesterase inhibitors. *Bioorg. Chem.* **2016**, *69*, 91–101. [[CrossRef](#)] [[PubMed](#)]
2. Auld, D.S.; Kornecook, T.J.; Bastianetto, S.; Quirion, R. Alzheimer's disease and the basal forebrain cholinergic system: Relations to β -amyloid peptides, cognition, and treatment strategies. *Prog. Neurobiol.* **2002**, *68*, 209–245. [[CrossRef](#)]
3. Adams, R.L.; Craig, P.L.; Parsons, O.A. Neuropsychology of dementia. *Neurol. Clin.* **1986**, *4*, 387–404. [[CrossRef](#)]
4. Giacobini, E. Cholinesterases: New roles in brain function and in Alzheimer's disease. *Neurochem. Res.* **2003**, *28*, 515. [[CrossRef](#)] [[PubMed](#)]
5. Holzgrabe, U.; Kapková, P.; Alptüzün, V.; Scheiber, J.; Kugelmann, E. Targeting acetylcholinesterase to treat neurodegeneration. *Expert Opin. Ther. Targets* **2007**, *11*, 161. [[CrossRef](#)]
6. Massoulié, J.; Pezzementi, L.; Bon, S.; Krejci, E.; Vallette, F.M. Molecular and cellular biology of cholinesterases. *Prog. Neurobiol.* **1993**, *41*, 31–91. [[CrossRef](#)]
7. Mushtaq, G.; Greig, N.H.; Khan, J.A.; Kamal, M.A. Status of acetylcholinesterase and butyrylcholinesterase in Alzheimer's disease and type 2 diabetes mellitus. *CNS Neurol. Disord. Drug Targets* **2014**, *13*, 1432–1439. [[CrossRef](#)]
8. Rahim, F.; Ullah, H.; Taha, M.; Wadood, A.; Javed, M.T.; Rehman, W.; Nawaz, M.; Ashraf, M.; Ali, M.; Sajid, M.; et al. Synthesis and in vitro acetylcholinesterase and butyrylcholinesterase inhibitory potential of hydrazide based Schiff bases. *Bioorg. Chem.* **2016**, *68*, 30–40. [[CrossRef](#)]
9. Wang, J.; Timchalk, C.; Lin, Y. Carbon nanotube-based electrochemical sensor for assay of salivary cholinesterase enzyme activity: An exposure biomarker of organophosphate pesticides and nerve agents. *Environ. Sci. Technol.* **2008**, *42*, 2688. [[CrossRef](#)] [[PubMed](#)]
10. Ullah, H.; Fayyaz, F.; Hussain, A.; Rahim, F.; Rehman, A.; Wadood, A.; Khan, K.M. New oxadiazole bearing thiosemicarbazide analogues: Synthesis, anti-alzheimer inhibitory potential and their molecular docking study. *Chem. Data Collect.* **2022**, *41*, 100915. [[CrossRef](#)]
11. Small, G.W.; Rabins, P.V.; Barry, P.P.; Buckholts, N.S.; Dekosky, S.T.; Ferris, S.H. Diagnosis and treatment of Alzheimer disease and related disorders. *J. Am. Med. Assoc.* **1997**, *278*, 1363–1371. [[CrossRef](#)]
12. Spasov, A.; Yozhitsu, I.N.; Bugaeva, L.I.; Anisimova, V.A. Benzimidazole derivatives: Spectrum of pharmacological activity and toxicological properties (a review). *Pharm. Chem. J.* **1999**, *33*, 232–243. [[CrossRef](#)]
13. Patil, A.; Ganguly, S.; Surana, S. A systematic review of benzimidazole derivatives as an antiulcer agent. *Rasayan. J. Chem.* **2008**, *1*, 447–460.
14. Dubey, K.; Sanyal, P.K. Benzimidazole sinawormyworld. *Vet Scan | Online Vet. Med. J.* **2010**, *5*, 63.
15. Boiani, M.; González, M. Imidazole and benzimidazole derivatives as chemotherapeutic agents. *Mini Rev. Med. Chem.* **2005**, *5*, 409–424. [[CrossRef](#)]
16. Narasimhan, B.; Sharma, D.; Kumar, P. Benzimidazole: A medicinally important heterocyclic moiety. *Med. Chem. Res.* **2012**, *21*, 269–283. [[CrossRef](#)]
17. Vishnuji, R.; Arun, S.; Mahendra, N.; Ramendra, P. *The Chemistry of Heterocycles: Nomenclature and Chemistry of Three-to-Five Membered Heterocycles*; Elsevier: Amsterdam, The Netherlands, 2019; pp. 149–478.
18. Bansal, Y.; Silakari, O.; Lapinsky, D.J.; Kusayanagi, T.; Tsukuda, S.; Shimura, S.; Manita, D.; Iwakiri, K.; Kamisuki, S.; Takakusagi, Y.; et al. The therapeutic journey of benzimidazoles: A review. *Bioorg. Med. Chem.* **2012**, *20*, 6199–6207. [[CrossRef](#)]
19. Parekh, N.M.; Juddhawal, K.V.; Rawal, B.M. Antimicrobial activity of thiazolyl benzenesulfonamide-condensed 2, 4-thiazolidinediones derivatives. *Med. Chem. Res.* **2013**, *22*, 2737–2745. [[CrossRef](#)]
20. Rostom, S.A.; El-Ashmawy, I.M.; AbdElRazik, H.A.; Badr, M.H.; Ashour, H.M. Design and synthesis of some thiazolyl and thiadiazolyl derivatives of antipyrine as potential non-acidic anti-inflammatory, analgesic and antimicrobial agents. *Bioorg. Med. Chem.* **2009**, *17*, 882–895. [[CrossRef](#)]
21. Haroun, M.; Tratat, C.; Tsolaki, E.; Geronikaki, A. Thiazole-based thiazolidinones as potent antimicrobial agents. Design, synthesis and biological evaluation. *Comb. Chem. High Throughput Screen* **2016**, *19*, 51–57. [[CrossRef](#)]
22. Luzina, E.L.; Popov, A.V. Synthesis and anticancer activity of N-bis (trifluoromethyl) alkyl-N'-thiazolyl and N-bis (trifluoromethyl) alkyl-N'-benzothiazolyl ureas. *Eur. J. Med. Chem.* **2009**, *44*, 4944–4953. [[CrossRef](#)] [[PubMed](#)]
23. Zablotskaya, A.; Segal, I.; Germane, S.; Shestakova, I.; Domracheva, I.; Nesterova, A.; Geronikaki, A.; Lukevics, E. Silyl modification of biologically active compounds. 8. Trimethylsilyl ethers of hydroxyl-containing thiazole derivatives. *Chem. Heterocycl. Compd.* **2002**, *38*, 859–866. [[CrossRef](#)]
24. Britschgi, M.; Greyerz, S.; Burkhart, C.; Pichler, W.J. Molecular aspects of drug recognition by specific T cells. *Curr. Drug Targets* **2003**, *4*, 1–11. [[CrossRef](#)] [[PubMed](#)]
25. Turan-Zitouni, G.; Chevallet, P.; Kilic, F.S.; Erol, K. Synthesis of some thiazolyl-pyrazoline derivatives and preliminary investigation of their hypotensive activity. *Eur. J. Med. Chem.* **2000**, *35*, 635–641. [[CrossRef](#)]
26. Mohsen, U.A.; Kaplancikli, Z.A.; Ozkay, Y.; Yurttas, E.L. Synthesis and evaluation of anti-acetylcholinesterase activity of some benzothiazole based new piperazine-dithiocarbamate derivatives. *Drug Res.* **2015**, *65*, 176–183. [[CrossRef](#)]
27. Yin, L.; Cheng, F.C.; Li, Q.X.; Liu, W.W.; Liu, X.J.; Cao, Z.L.; Shi, D.H. Synthesis and biological evaluation of novel C1-glycosyl thiazole derivatives as acetylcholinesterase inhibitors. *J. Chem. Res.* **2016**, *40*, 545–548. [[CrossRef](#)]

28. Wang, Y.X.; Liu, S.H.; Shao, Z.B.; Cao, L.G.; Jiang, K.J.; Lu, X.; Wang, L.; Liu, W.W.; Shi, D.H.; Cao, Z.L. Synthesis and anti-acetylcholinesterase activities of novel glycosyl coumarylthiazole derivatives. *J. Chem. Res.* **2021**, *2021*, 359–364. [[CrossRef](#)]
29. Ibrar, A.; Zaib, S.; Khan, I.; Jabeen, F.; Iqbal, J.; Saeed, A. Facile and Expedient Access to Bis-Coumarin–Iminothiazole Hybrids by Molecular Hybridization Approach: Synthesis, Molecular Modelling and Assessment of Alkaline Phosphatase Inhibition, Anticancer and Antileishmanial Potential. *RSC Adv.* **2015**, *5*, 89919–89931. [[CrossRef](#)]
30. Haroon, M.; Khalid, M.; Shahzadi, K.; Akhtar, T.; Saba, S.; Rafique, J.; Ali, S.; Irfan, M.; Alam, M.M.; Imran, M. Alkyl 2-(2-(arylidene) alkylhydrazinyl) thiazole-4-carboxylates: Synthesis, acetyl cholinesterase inhibition and docking studies. *J. Mole. Stru.* **2021**, *1245*, 131063. [[CrossRef](#)]
31. Chhabria, M.; Patel, S.; Modi, P.; Brahmshatriya, P. Thiazole: A review on chemistry, synthesis and therapeutic importance of its derivatives. *Curr. Top. Med. Chem.* **2016**, *16*, 2841–2862. [[CrossRef](#)]
32. Taha, M.; Ullah, H.; AlMuqarrabun, L.M.R.; Khan, M.N.; Rahim, F.; Ahmat, N.; Ali, M.; Perveen, S. Synthesis of bis-indolylmethanes as new potential inhibitors of β -glucuronidase and their molecular docking studies. *Eur. J. Med. Chem.* **2018**, *143*, 1757–1767. [[CrossRef](#)] [[PubMed](#)]
33. Taha, M.; Sultan, S.; Nuzar, H.A.; Rahim, F.; Imran, S.; Ismail, N.H.; Naz, H.; Ullah, H. Synthesis and biological evaluation of novel N-arylidenequinoline-3-carbohydrazides as potent β -glucuronidase inhibitors. *Bioorg. Med. Chem.* **2016**, *24*, 3696–3704. [[CrossRef](#)] [[PubMed](#)]
34. Taha, M.; Javid, M.T.; Imran, S.; Selvaraj, M.; Chigurupati, S.; Ullah, H.; Rahim, F.; Khan, F.; Mohammad, J.I.; Khan, K.M. Synthesis and study of the α -amylase inhibitory potential of thiadiazole quinoline derivatives. *Bioorg. Chem.* **2017**, *74*, 179–186. [[CrossRef](#)]
35. Rahim, F.; Ullah, K.; Ullah, H.; Wadood, A.; Taha, M.; Rehman, A.; Din, I.U.; Ashraf, M.; Shaukat, A.; Rehman, W.; et al. Triazinoindole analogs as potent inhibitors of α -glucosidase: Synthesis, biological evaluation and molecular docking studies. *Bioorg. Chem.* **2015**, *58*, 81–87. [[CrossRef](#)] [[PubMed](#)]
36. Taha, M.; Rahim, F.; Imran, S.; Ismail, N.H.; Ullah, H.; Selvaraj, M.; Javid, M.T.; Salar, U.; Ali, M.; Khan, K.M. Synthesis, α -glucosidase inhibitory activity and in silico study of tris-indole hybrid scaffold with oxadiazole ring: As potential leads for the management of type-II diabetes mellitus. *Bioorg. Chem.* **2017**, *74*, 30–40. [[CrossRef](#)]
37. Rahim, F.; Ullah, H.; Javid, M.T.; Wadood, A.; Taha, M.; Ashraf, M.; Shaukat, A.; Junaid, M.; Hussain, S.; Rehman, W.; et al. Synthesis, in vitro evaluation and molecular docking studies of thiazole derivatives as new inhibitors of α -glucosidase. *Bioorg. Chem.* **2015**, *62*, 15–21. [[CrossRef](#)]
38. Rahim, F.; Malik, F.; Ullah, H.; Wadood, A.; Khan, F.; Javid, M.T.; Taha, M.; Rehman, W.; Rehman, A.U.; Khan, K.M. Isatin based Schiff bases as inhibitors of α -glucosidase: Synthesis, characterization, in vitro evaluation and molecular docking studies. *Bioorg. Chem.* **2015**, *60*, 42–48. [[CrossRef](#)]
39. Rahim, F.; Ali, M.; Ullah, S.; Rashid, U.; Ullah, H.; Taha, M.; Javed, M.T.; Rehman, W.; Abid, O.U.R.; Khan, A.A.; et al. Development of bis-thiobarbiturates as successful urease inhibitors and their molecular modeling studies. *Chin. Chem. Lett.* **2016**, *27*, 693–697. [[CrossRef](#)]
40. Rahim, F.; Zaman, K.; Ullah, H.; Taha, M.; Wadood, A.; Javed, M.T.; Rehman, W.; Ashraf, M.; Uddin, R.; Uddin, I.; et al. Synthesis of 4-thiazolidinone analogs as potent in vitro anti-urease agents. *Bioorg. Chem.* **2015**, *63*, 123–131. [[CrossRef](#)]
41. Taha, M.; Ullah, H.; AlMuqarrabun, L.M.R.; Khan, M.N.; Rahim, F.; Ahmat, N.; Javid, M.T.; Ali, M.; Khan, K.M. Bisindolylmethane thiosemicarbazides as potential inhibitors of urease: Synthesis and molecular modeling studies. *Bioorg. Med. Chem.* **2018**, *26*, 152–160. [[CrossRef](#)]
42. Adalat, B.; Rahim, F.; Taha, M.; Alshamrani, F.J.; Anouar, E.H.; Uddin, N.; Shah, S.A.A.; Ali, Z.; Zakaria, Z.A. Synthesis of Benzimidazole-Based Analogs as Anti Alzheimer's Disease Compounds and Their Molecular Docking Studies. *Molecules* **2020**, *25*, 4828. [[CrossRef](#)] [[PubMed](#)]
43. Rahim, F.; Javed, M.T.; Ullah, H.; Wadood, A.; Taha, M.; Ashraf, M.; Khan, M.A.; Khan, F.; Mirza, S.; Khan, K.M. Synthesis, molecular docking, acetylcholinesterase and butyrylcholinesterase inhibitory potential of thiazole analogs as new inhibitors for Alzheimer disease. *Bioorg. Chem.* **2015**, *62*, 106–116. [[CrossRef](#)] [[PubMed](#)]
44. Mekky, E.M.; Sanad, S.M.; El-Idreesy, T.T. New thiazole and thiazole-chromene hybrids possessing morpholine units: Piperazine-mediated one-pot synthesis of potential acetylcholinesterase inhibitors. *Synth. Commun.* **2021**, *51*, 3332–3344. [[CrossRef](#)]
45. Hemaida, A.Y.; Hassan, G.S.; Maarouf, A.R.; Joubert, J.; El-Emam, A.A. Synthesis and Biological Evaluation of Thiazole-Based Derivatives as Potential Acetylcholinesterase Inhibitors. *ACS Omega* **2021**, *6*, 19202–19211. [[CrossRef](#)] [[PubMed](#)]
46. Rahim, F.; Zaman, K.; Taha, M.; Ullah, H.; Ghufuran, M.; Wadood, A.; Rehman, W.; Uddin, N.; Shah, S.A.A.; Sajid, M.; et al. Synthesis, invitro α -glucosidase inhibitory potential of benzimidazole bearing bis-Schiff bases and their molecular docking study. *Bioorg. Chem.* **2020**, *94*, 103394. [[CrossRef](#)]
47. Cacabelos, R. Donepezil in Alzheimer's disease: From conventional trials to pharmacogenetics. *Neuropsychiatr. Dis. Treat.* **2007**, *3*, 303–333.
48. Wadood, A.; Shareef, A.; Rehman, A.U.; Muhammad, S.; Khurshid, B.; Khan, R.S.; Shams, S.; Afridi, S.G. In silico drug designing for ala438 deleted ribosomal protein S1 (RpsA) on the basis of the active compound Zrl 15. *ACS Omega* **2022**, *7*, 397–408. [[CrossRef](#)]
49. Rehman, A.U.; Zhen, G.; Zhong, B.; Ni, D.; Li, J.; Nasir, A.; Gabr, M.T.; Rafiq, H.; Wadood, A.; Lu, S.; et al. Mechanism of zinc ejection by disulfiram in nonstructural protein 5A. *Phys. Chem. Chem. Phys.* **2021**, *23*, 12204–12215. [[CrossRef](#)]

50. Chigurupati, S.; Selvaraj, M.; Mani, V.; Selvarajan, K.K.; Mohammad, J.I.; Kaveti, B.; Bera, H.; Palanimuthu, V.R.; Teh, L.K.; Salleh, M.Z. Identification of novel acetylcholinesterase inhibitors: Indolopyrazoline derivatives and molecular docking studies. *Bioorganic Chem.* **2016**, *67*, 9–17. [[CrossRef](#)]
51. Chigurupati, S.; Selvaraj, M.; Mani, V.; Mohammad, J.I.; Selvarajan, K.K.; Akhtar, S.S.; Marikannan, M.; Raj, S.; Teh, L.K.; Salleh, M.Z. Synthesis of azomethines derived from cinnamaldehyde and vanillin: In vitro aetylcholinesterase inhibitory, antioxidant and insilico molecular docking studies. *Med. Chem. Res.* **2018**, *27*, 807–816. [[CrossRef](#)]